ISSN 0970 - 4477

WRI JOURNAL

October - December 2017 Journal of the Welding Research Institute Vol : 38 No. : 4

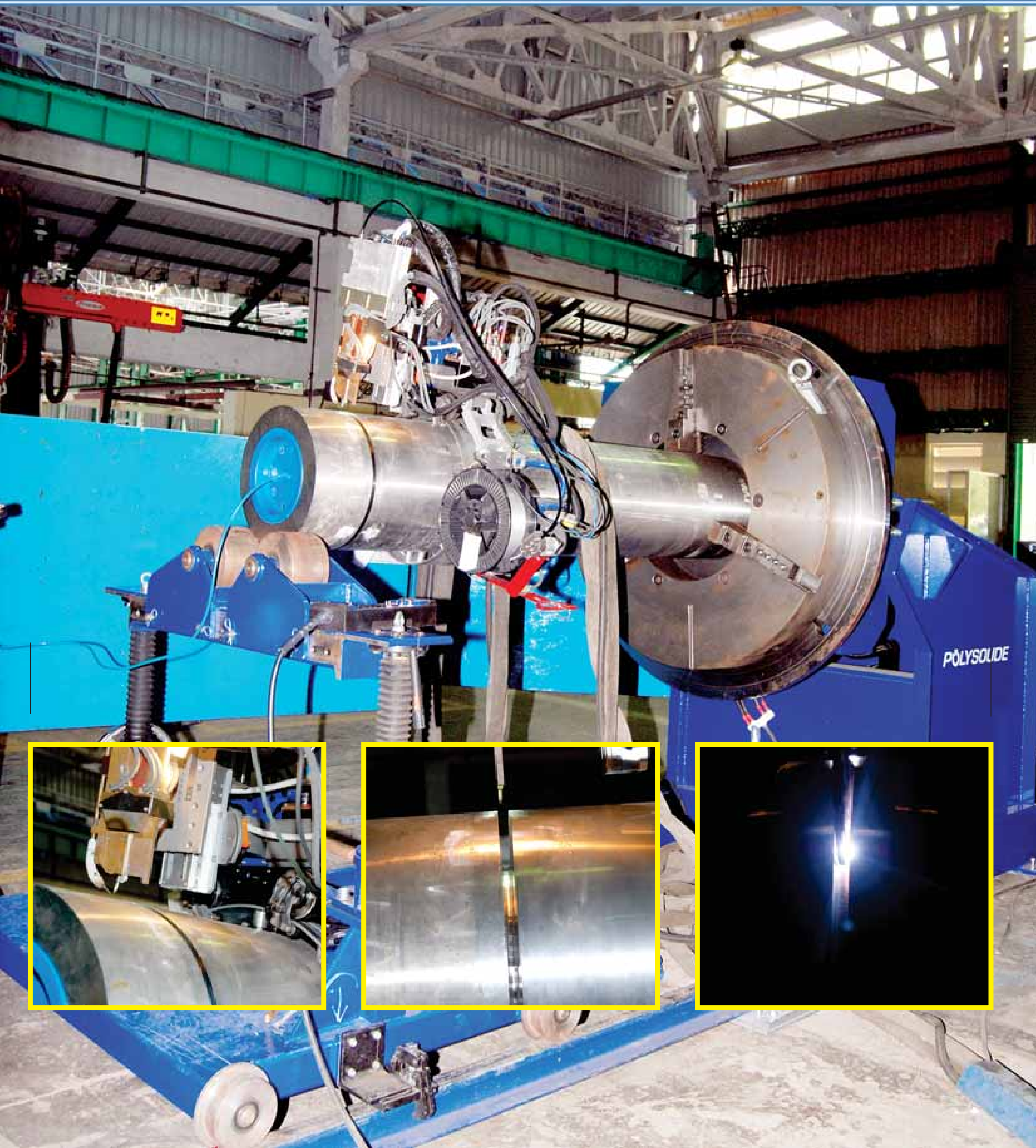

AWARDS AND RECOGNITIONS

NMD-ATM 2017 - METALLOGRAPHY CONTEST

Dr. K. Devakumaran, DM/WRI and his team have won the first prize in the Metallography Contest in both Optical and SEM categories for the images captured in the dissimilar weld between P92 and Super 304H stainless steel using Alloy 52M filler wire. The images that won their team the first prize are given below

Oxide's Spinning Wheel :

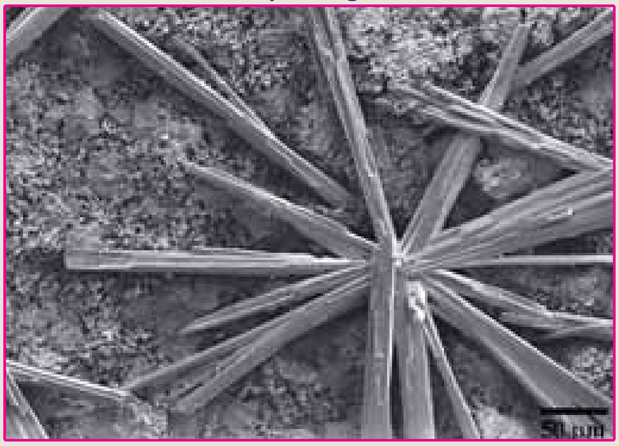

Hitters in the Waves of the Sea Coast...

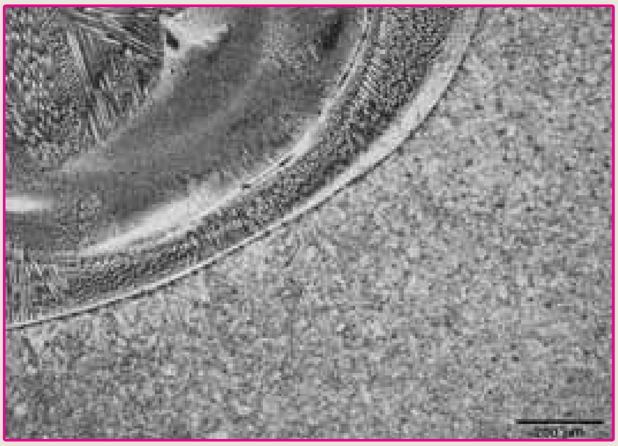

Basc Metal - T92 : Weld Metal - IN 52M
Etchant:
T92- Vilella's reagent (T92) and
IN 52M- 10% Oxalie acid (Electrolytic etching)

Incidentally, Dr. K. Devakumaran has bagged the first prize for the second time. This reiterates the capability of WRI in metallurgical analysis of welds.

NATIONAL SAFETY AWARD

WRI has own (Runner) the coveted National Safety Awards for the performance Year 2015 in both Lowest Average Frequency Rate and Longest Accident Free Period categories. National Safety Awards are instituted by Govt. of India to recognize the industrial undertakings that are adopting best safety practices and for implementation jointly by Management and Employees. BHEL, Trichy has received the maximum awards for the year 2015. The awards were handed over by the Hon'ble' Minister of State for Labour & Employment, Govt. of India, Shri. Santosh Kumar Gangwar. The awards were received by Shri. R. Rajamanohar, Executive Director, BHEL, Trichy and was later presented to WRI. Dr. B. Shanmugarajan, SM/WRI received the award from the Executive Director on behalf of General Manager, WRI & Labs.

CONTENTS

WRI JOURNAL

October - December 2017 Vol 38 - No.4

TECHNICAL PAPERS

OTHER FEATURES

COVER PAGES

Edited & Published by
R. Subbarayalu
for and on behalf of
Welding Research Institute
Tiruchirappalli - 620 014
India

For Details Contact:
Editor - WRI Journal
Welding Research Institute
Bharat Heavy Electricals
Limited

www.wriindia.com

Publisher's Information

WRI Journal is available to individuals and organisations on subscription basis @ Rs. 2000 for four consecutive issues in India and @ US $ 100 for overseas by Airmail.

System Designed & Printed at
Poornima Printers
Bengaluru - 560 040
Email : poornipr@gmail.com
Off: + 080-23359588

Editorial

Dear Reader,

Greetings from Welding Research Institute - India!

With the never ending support given by the top management of BHEL, Govt. of India at appropriate times and invaluable customers of the institute, on November 01, 2017, Welding Research Institute is stepping into the forty third year of service to the welding fraternity and the nation at large. With the facility up gradation going on in full swing through the Govt. of India sanctioned Advanced Ultra Super Critical (AUSC) project, it is indeed a special birthday for WRI! At this juncture, as The Head of the institute, I take immense pleasure in thanking all for the faith and confidence shown towards the institute from time to time in the glorious journey all these years. I request all to extend the same kind of support in the coming years. From our end, I assure you of our best services at all times.

The period Oct - Dec 2017 had been sweetly busy with various activities like development of process/applications for the prestigious national mission project for development of AUSC technology, placement of purchase orders for procurement of state-of-art facilities in welding and weld characterisation, etc. During this period, a workshop on 'Revolution in Header to Stub Welding' had been organised at WRI. Mr. Prabhu Nallathambi from M/s Ayyappa Welding Services delivered the talk highlighting the developments. It is heartening to see the team from WRI bagging the First Prize in Metallography Contest organised as part of NMD and WRI securing the runners up trophy in the National Safety Awards for the year 2015. WRI had also marked its presence in the R&D and academics with WRI executives giving lectures/presentations in different forums in various events/conferences organised across the country.

In this issue, we have put together three articles. Here is a short preview for you:

Understanding the characteristics of the welding power source will be helpful in controlling the arc behaviour thereby controlling the defects at the origin. The first article discusses the results of modeling and simulation studies carried out for a SMAW power source.

Distortion is a nuisance and the best way to solve it is to avoid it totally from occurring. The second article studies the usefulness of the available empirical formulas in predicting the longitudinal bending distortion in one sided fillet joints by comparing with the experimental values.

The third article gives an insight on the practical application of a waveform control technology for welding header to stub joints.

We expect this would be useful and informative to a wide range of our readers. Remember to send your feedback to help improve this Journal further.

With Best Regards

R. Subbarayalu

MODELING AND SIMULATION STUDIES ON ARC WELDING POWER SOURCE

P. R. Venkateswaran, Thomas P Rajan*, Sundareswaran*

Welding Research Institute, BHEL, Tiruchirappalli 620014
**National Institute of Technology, Tiruchirappalli 620015*

Abstract: *Arc welding power sources provide a nonlinear design and dynamics that do not provide a comprehensive understanding of the arc phenomena. Hence, it is important to understand the arc behaviour by modeling of the system and match it with simulated results to validate the model. Since welding arc behaviour is also dynamic in nature, it is difficult to approximate the welding process behaviour with sufficient accuracy. It is proposed to simulate a shielded metal arc welding process with a mathematical model inducing non linearity through arc length and arc disturbances. Thus the developed model offers a chance to be a prototype, which could be used for understanding the process and arc behaviour under different set of non-linearity present in the working environment. The simulated results show that the model is capable of closely resembling an inverter based power source faithfully and thereby providing a prototype for design and experimental studies on the characteristics of a welding power source. It is possible to custom design a power source for achieving the design characteristics. This simulation study discusses the background of the typical building blocks of the welding power source, mathematical modeling of a manual welding power source, simulation results of the model, analysis of the model under different operating conditions of induced disturbances and application of the model for design and experimental studies.*

Keywords**: **Arc welding power source model, dynamic characteristics, arc modeling, welding process disturbances.

1.0 Introduction

The functional requirement of an arc welding power source is to deliver the rated values of voltage and current to the welding process. In that aspect, it can be visualized that all power sources retain the same purpose and characteristic behaviour. Power sources are fabricated using multiple types of designs [1] to deliver the rated values as output. It is expected that the power source design be robust to deliver the rated values inspite of process and environmental disturbances. The ability of the designer to verify this output requirement is constrained due to the need to consider simulation of the output under different operating condition with a valid mathematical model. The disturbances influencing the power source output include load variations, temperature in the welding environment, operating range of the design elements, process disturbances like arc length fluctuations and arc blow. These factors make the definition of welding as a nonlinear process, as the relation between input and output are not governed by a linear relation. In this paper, a Shielded Metal Arc Welding (SMAW) power source is considered for simulation in which the process and environmental disturbances are included both from theoretical and practical experience. The SMAW process was converted into an electrical model [2] and simulated on a software platform with controller. The ability of the design to produce the rated output in the presence of disturbances was evaluated for different types of disturbances. Section 2.0 details the features of the SMAW process model and operating parameters considered for simulation studies. It also details the background of the choice of the component values chosen for the SMAW model circuit. Section 3.0 describes the dynamic load modeling of the power source built on MATLAB platform and the choice of simulation parameters. Section 4.0 dwells on the controller function for the power source and explains the role of a typical PI controller for the model. Section 5.0 seeks to analyze and comment on the output of the SMAW model and how it meets the process requirements.

2.0 SMAW process as electrical circuit model

SMAW process uses a consumable electrode to join two metal pieces by a weld. The energy required to weld the joints is provided by the electrically enabled arc discharge between the electrode and the work piece. The process has different working parts attributable to mechanical, electrical, metallurgical domain functions. For the purpose of modeling the process, it is proposed to consider the SMAW process as an electrical circuit [2], [3] in which a source delivers the rated power to the load through a closed circuit. The electrical characteristic considered for the power source is a constant current characteristic as shown in Fig. 1. The modeled power source is expected to deliver output rated current with minimum deviation in spite of all the process and environmental disturbances. This is taken as a fundamental output requirement for the model proposed in this paper. The model referenced by [2] is taken up for simulation studies with difference in the assigned values for parameters. This model translates the function of a power source in stages generically. The choice of operating parameters is dictated by the practical considerations of the value of Open Circuit Voltage (OCV), permissible deviation in the output current, design values of the individual electronic components like diodes, MOSFETs considered for use. The expression for arc voltage for a typical electrical model of the SMAW circuit for a stable arc is given by [4] as

$$V_{arc} = V_c + V_A + El_{arc} + R_a I_a \qquad (1)$$

Where V_c is cathode voltage drop, V_A is anode voltage drop, l_{arc} is length of the arc, E is arc length factor (Electric field intensity), and R_a is the resistance associated with the arc. The arc voltage in practice is a function of each of the operating point, types of consumable used and the prevalent process conditions. This non linearity is to be sufficiently reflected in the choice of the values associated with the equation (1). For a constant current characteristic assumed for this model, the skill of the welder plays an important role and should sufficiently be included in the amplitude of these values. If I_{arc} is held constant, it will sufficiently ensure arc stability in spite of all process and environmental disturbances.

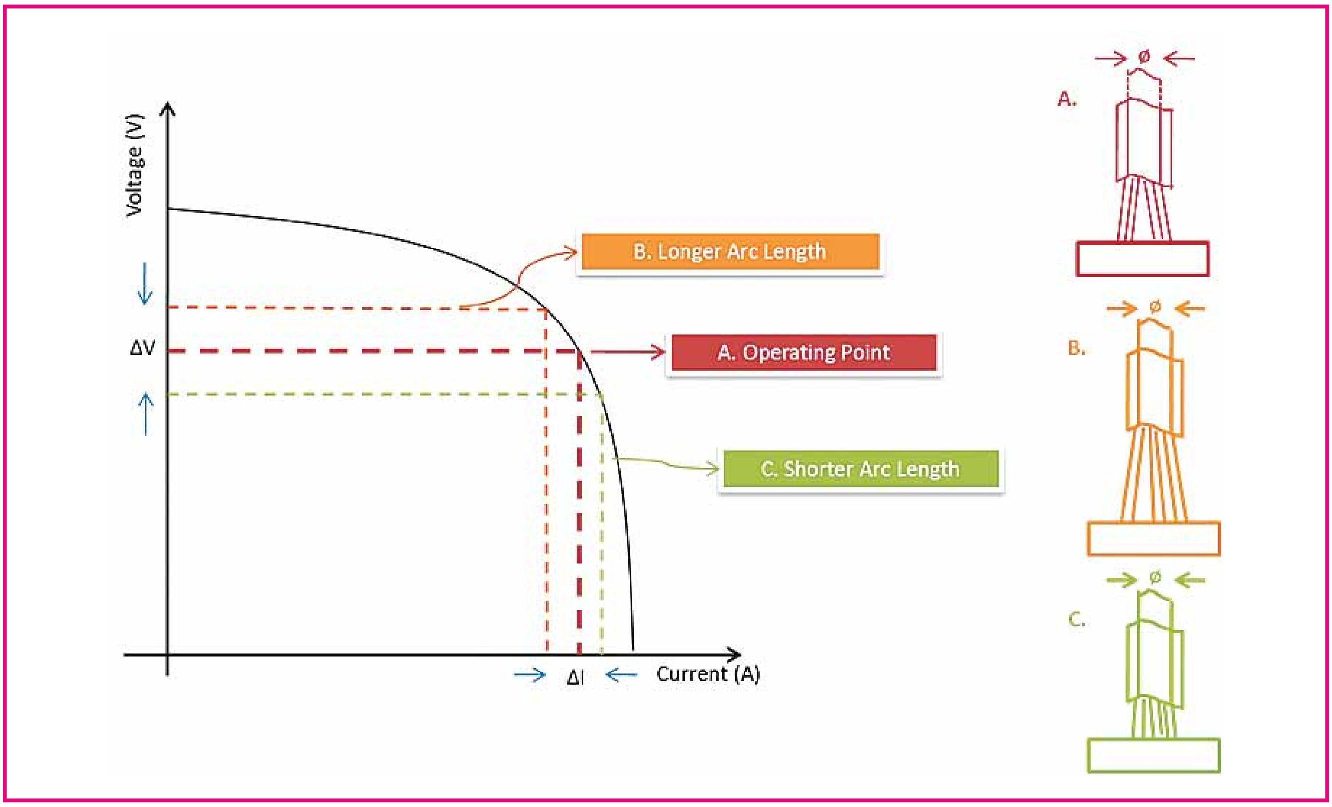

Figure 1 - Constant current characteristic of the welding power source

The power source design that is considered for simulation is an Inverter based design. The model [4] resembles therefore, has to convert the input supply to steady state DC using a rectifier. The SMAW process model is visualized electrically as in Fig. 2 and goes through the stages of rectifier, filters, MOSFET switching, transformer for step up/step down, cable resistance and inductance and closed with the electrode and weld specimen. The first stage in the model is to convert the input three phase supply to the DC. The inversion will be followed by a high frequency switching mechanism to convert the DC to AC. Subsequently, the AC value could be scaled by using a transformer before delivering the output at rated values to the welding circuit. Hence,it is important to include all impedance that will impact the electrical circuit towards the generation of output voltage. Considering those parameters, the open circuit voltage of the full bridge rectifier circuit of the power source model is given by

$$V_{oc} = \left(L_f + L_c\right)\frac{di_a}{dt} + (R_s + R_c)i_a + V_{arc} \quad \text{———} \quad (2)$$

Where R_a is the resistance of the welding loop, L_c and R_c are cable parameters, L_f is the inductance associated with the electrical circuit in the schematic diagram. The electrical model is divided into two parts. The section from the input supply till the physical output of the power source is identified as the electrical circuit and the load offered to this electrical circuit by the welding process through the connecting cables and work piece is identified as the welding circuit. The inductance and resistance in the welding circuit is identified as L_c and R_c respectively. It is practically not possible to measure V_{arc} and hence, an equivalent of V_{arc} in the form of V_{MT} is measured at the output terminals, as indicated assuming that the resistance and inductance of the cable are considered to be of small magnitude. The process of welding is highly nonlinear and the variations induced in these parameters are prone to high levels of variations that cannot be mapped in an equation form. Hence, the scope of modeling will be limited to successful generation of rated output current in spite of continuous process disturbances. The design of the controller, therefore, is limited to the stated provision in this model.

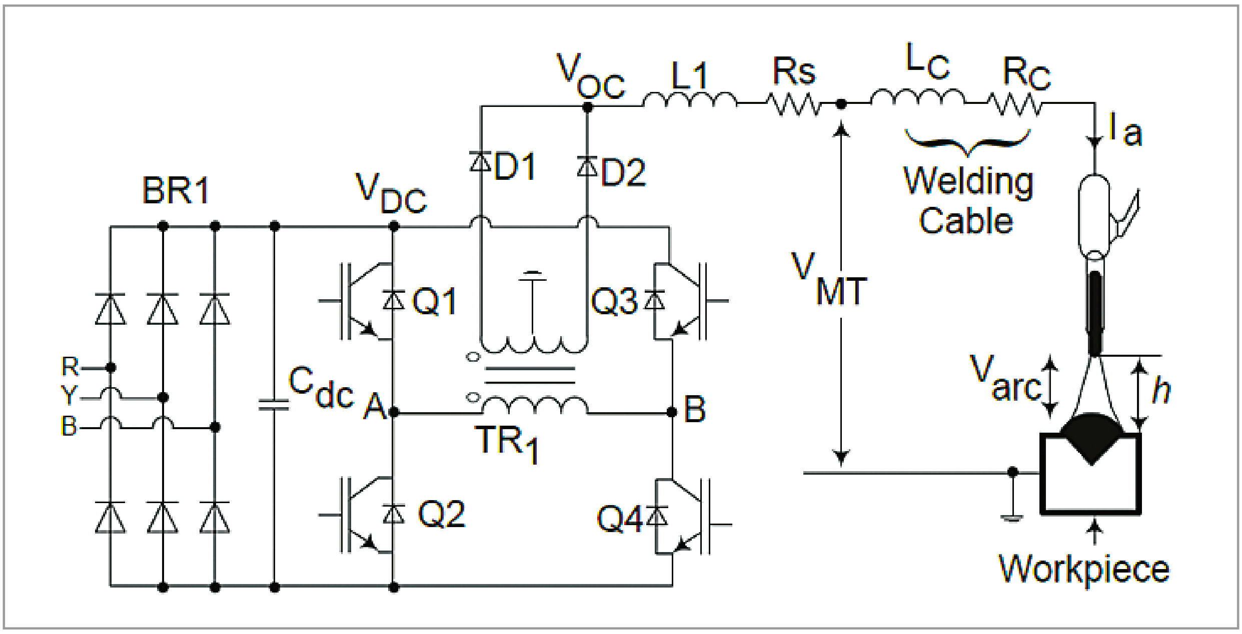

Figure 2 - Electrical model of SMAW process

Substituting for the value of V_{arc} in (2) from (1), we get

$$V_{oc} = (L_f + L_c)\frac{di_a}{dt} + (R_s + R_c)i_a + V_c + V_C + V_A + Eh + R_a i_a \quad \text{———} \quad (3)$$

This equation (3) is identified as the load model for the process and the current i_a is given by

$$i_a = \int \frac{V_{oc} - \left((R_s + R_c)i_a + V_c + V_C + V_A + Eh + R_a i_a\right)}{(L_f + L_c)}\, dt \quad \text{———} \quad (4)$$

It can be seen that the term is figuring in both left hand side and right hand side of the equation and hence, the result cannot be obtained by simple hand calculation. A simulation model which employs an iterative procedure will be needed for getting the results. The parameters mentioned in (4) are all assumed to reasonably follow a real life inverter based power source output to be compared with simulation. This makes the hypothesis of this paper that a real time simulated model can be made functionally available for all parametric variations where the operating range of the output current i_a will be faithfully represented by (4). This equation represents the dynamics of the operating current with respect to the fluctuations of the load operating on the circuit and hence, is called the load model. Since the model also represents the welding current output, the load model is deemed representing a controlled current source for the welding application.

3.0 Dynamic load model parameters and simulation:

The dynamic load model for the SMAW power source is based on varying the parameters of arc length, electric field intensity, anode and cathode drop, inductance of the welding loop, cable inductance and resistance. All these values are unpredictable in process flow and hence will be randomly varied in the model and the output will be studied. The limitations of this dynamic model are that the load or the loading pattern is not unique, parameters highly nonlinear, efficiency of operator, and large current fluctuations during short circuiting events. The typical measured voltage drop in the 50 mm^2 welding cable over a length of 10 m is given to be 0.35 V for every 100 A for inverter based power sources. The voltage drop due to the welding cable was approximated for a length of 2.5 m with these estimates. The model corresponding to equation (4) representing a constant current controlled power source was built on the Matlab Simulink Platform and is given in Fig. 3.

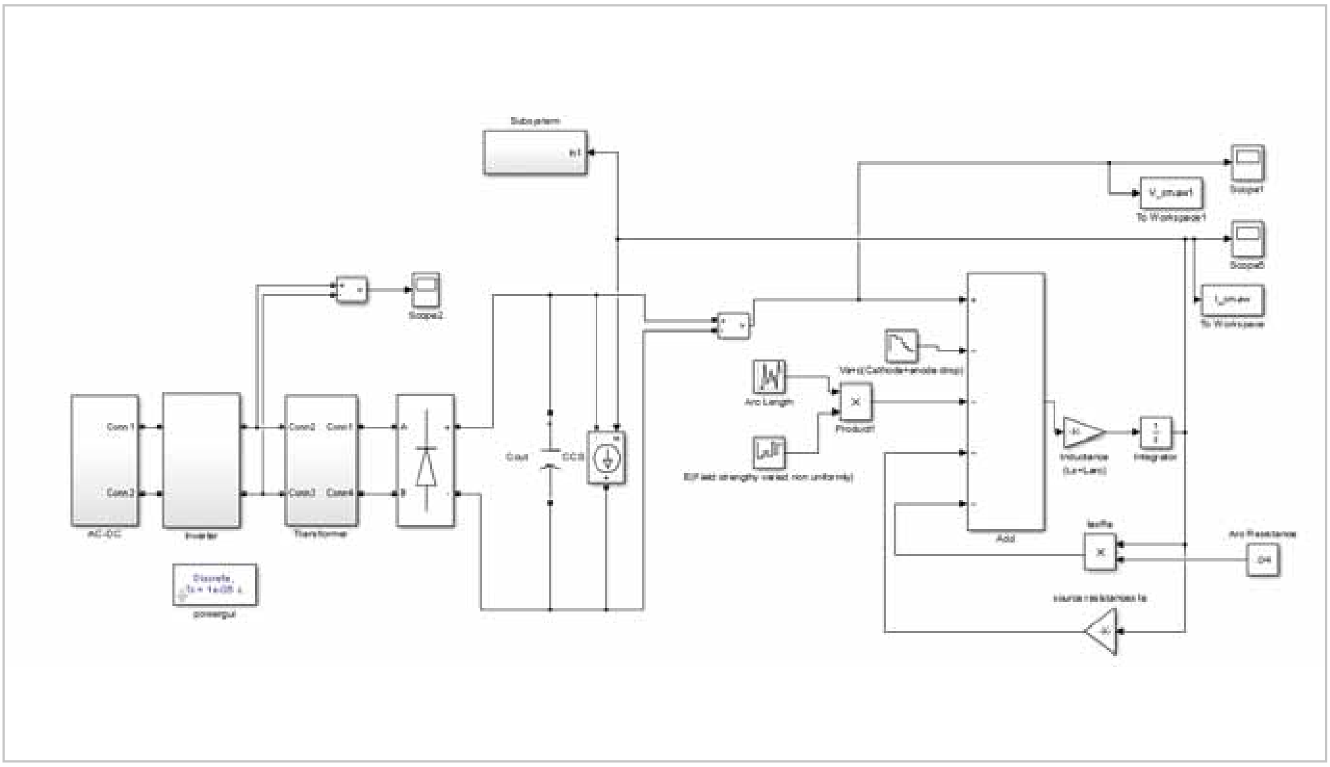

Figure 3 - Dynamic load model of SMAW power source in matlab platform

The Simulation Parameters for this model are presented in Table 1.

Table 1 - Simulation parameters for dynamic load model

Parameter	Value
Inverter switching frequency	10 kHz
Arc resistance	0.04 Ω
Inductance of the welding loop	10 µH
Filter capacitance	1000 µF
Source resistance	0.135 Ω
Source inductance	40 µH
Arc length variation	0 to 1 cm
Electric field intensity	250 to 300 V/m

The values given in Table 1 are typical values, which are normally found in a welding system. The reasons for the wise fluctuations are the uneven electrode tip, accidental short circuiting etc. The fluctuation in any one parameter will have a chain effect on the other parameters and hence, it may not be possible to study the variations in operating conditions with a simple equation. The analysis can best be carried out using matlab, which can carry out the analysis using several building blocks and deliver the output value of the arc current. The analysis has been carried out for a typical welding condition and the results are analyzed.

4.0 Controller model and functions

The reference value for control action in the power source will be the error generated between the reference value of current (set value for power source output) and the instantaneous value of the current output designated as i_a. The control action will be implemented through a Proportional Integral Derivative (PID) controller whose governing equation is given by

$$u(t) = K_p e(t) + K_I \int e(t)dt + K_d \frac{de(t)}{dt} \qquad (5)$$

Where u(t) is controller output and K_p, K_I and K_D are constants associated with proportional, integral and derivative control actions associated with the error e(t). In order to keep the deviations from average output value to minimum, the derivative action is minimized to zero. Hence, effectively, the controller action will be proportional integral only with integral constant kept at value to minimize the oscillations around set point.

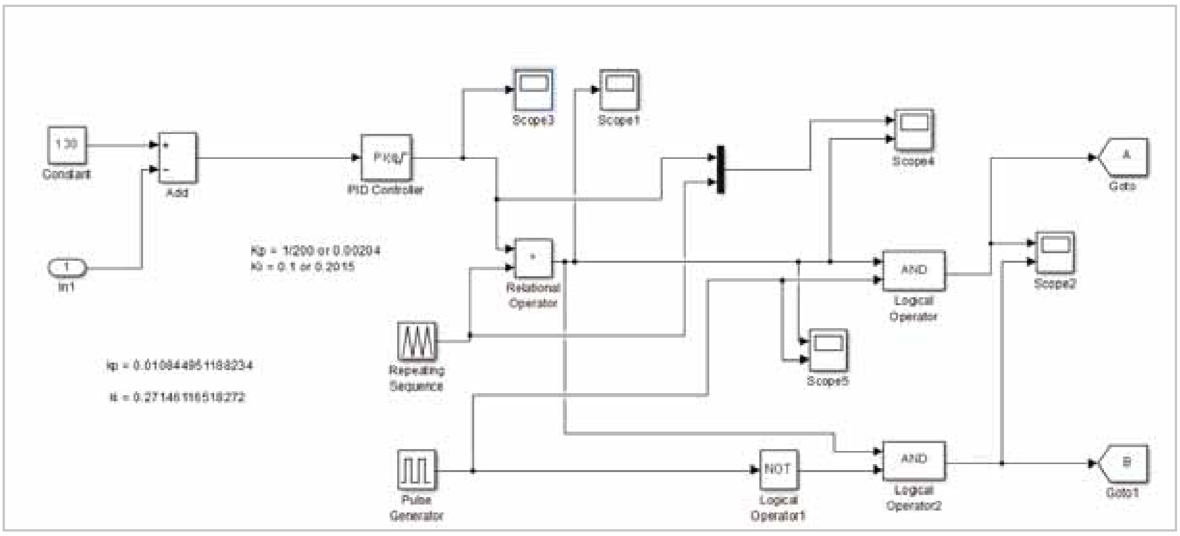

Figure 4 - PID Controller implementation in matlabplatform

The controller is a sub set of the load model but is extrapolated to reflect the importance of the working principle of the arc welding power source. The controller action is seen as a two stage operation. If and when the output current falls below the set value, an error is generated, which derives a corresponding output signal from the PID controller. The control signal shapes the PWM pulse output. The duration of the PWM pulse is the time during which the output is activated with the designated frequency. The frequency of the control signal decides the smoothness of the output. It is relevant to recall the flow of design in an inverter based power source to understand this control signal. A sine wave or square wave oscillator is usually used to convert the rectified, or battery dc voltage to a higher frequency. A PWM (pulse width modulated) controller may be used to regulate how the MOSFET, power transistor or thyristor is turned on and off by the oscillator signal. The pulse width modulation (PWM) modifies the duty cycle of a fixed switching frequency and thus control the time the device stays on or off.

Inverter switching is the next critical component of the power source design. The rate at which the DC voltage is switched on and off during the pulse width modulation process in a switching power supply. It can range from a few kHz to a few MHz. The choice will decide on the component sizing and weight of the physical construction of the welding power source. The selected frequency of switching will be executed in intervals of the duration of the pulses initiated by the control signal. This is indicated in Fig. 6. A wide range of switching frequencies is used in converter circuits based on the output voltage and sometimes the load and the available space. The balance between all these factors will decide on the specifications to select components with the ability to handle the design frequency. Since the physical fabrication is not intended to be the extension of the design, the goal of the controller signal is restricted to initiation of controller signal and choice of inverter switching frequency to the extent of achieving the constant current output in the presence of the disturbances. It is seen from Fig. 5. and Fig. 6., that the proposed model is able to generate control pulses and inverter switching frequencies at the selected values in the presence of process disturbances.

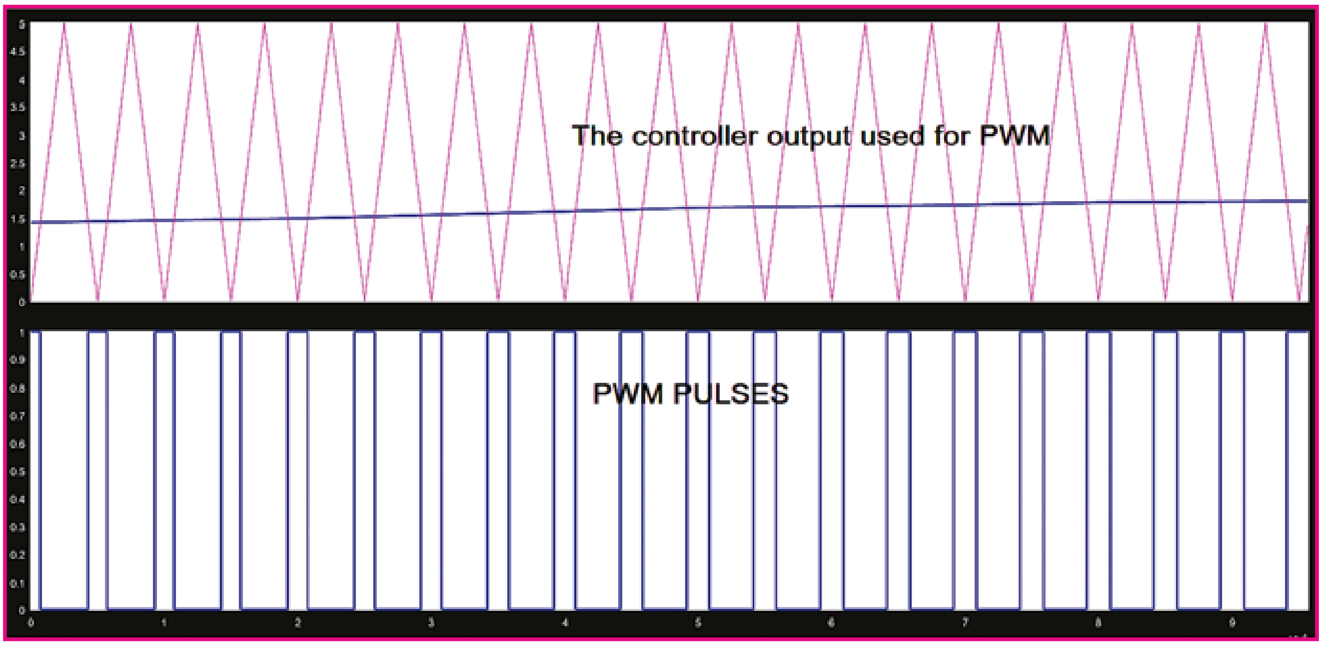

Figure 5 - Controller output in the form of PWM pulses

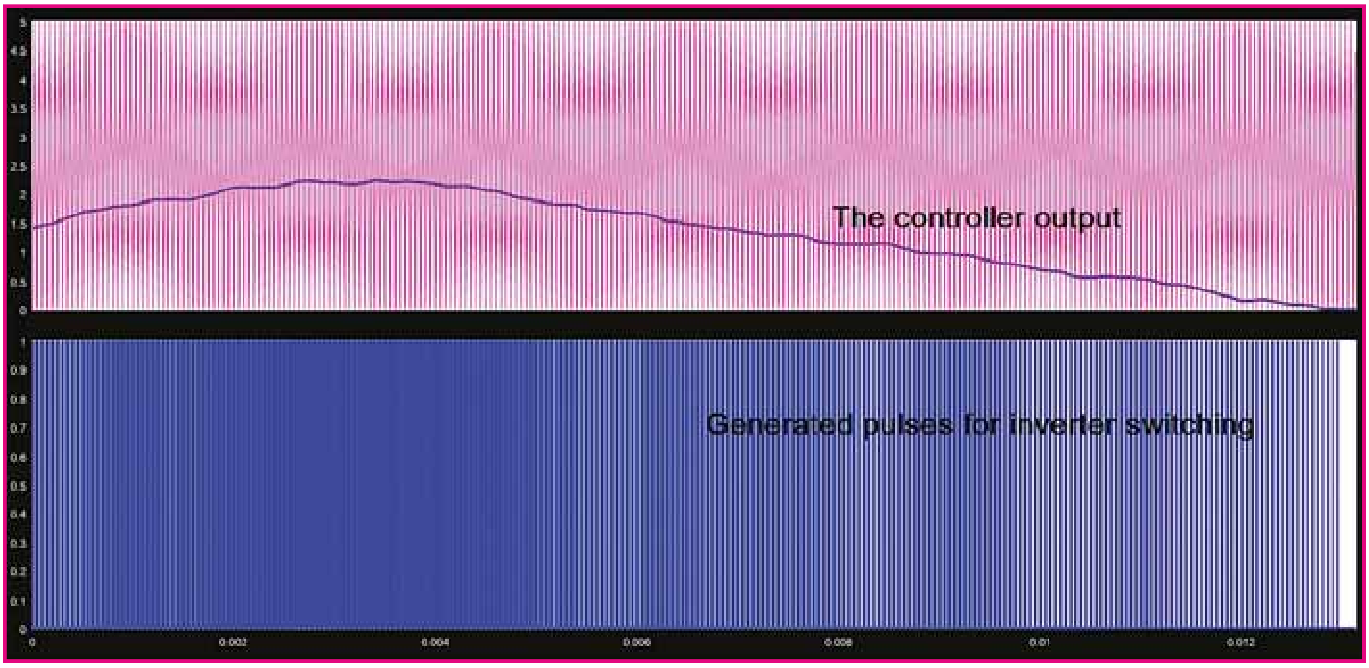

Figure 6 - Controller output for inverter switching of the DC to AC conversion

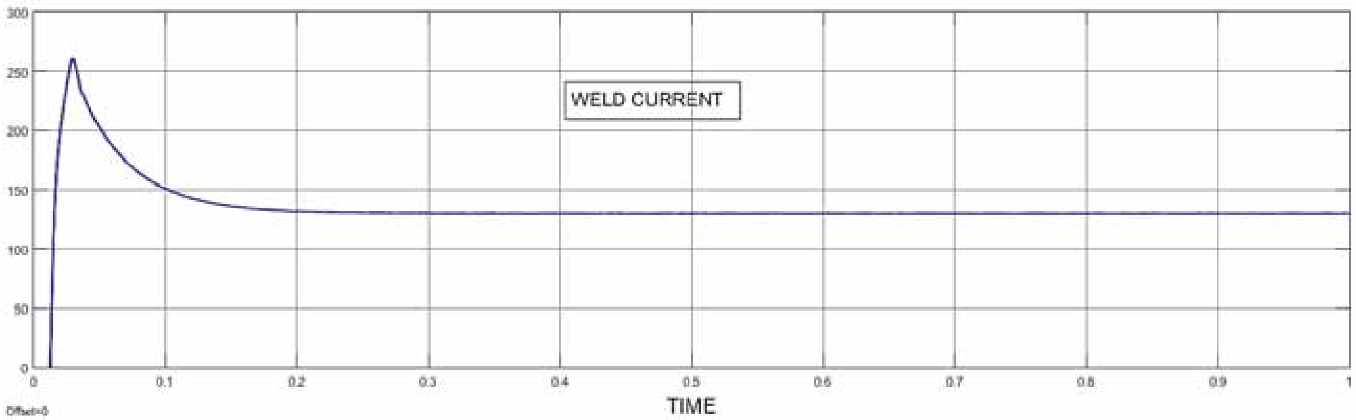

Figure 7 - Current output from the power source model with no disturbances

5.0 Results and Discussion

The power source model was assigned with the output target current of 130 A and the simulated output results are shown in Fig. 7 and Fig. 8 for current and voltage separately. As the load model is derived only for current as output, the voltage will be the derivative and will follow the current and will not have any separate control setting. These figures show an ideal situation of a simulation of a circuit, when the disturbances are considered to be NIL. It is fairly easy to generate an output under minimal disturbances, as the non-linearity gets to a fixed number and/or removed from the governing equation. Still, under consideration of the equations modeled for the power source, the characteristics obtained through Fig. 7 and Fig. 8 correspond to the typical output profile and delivers the expected output margins. The output waveforms thus correspond to the ideal situation of a stable arc length over entire weld region.

The dynamics are now introduced into the system by providing a range of values for electric field intensity, source resistance and inductance, arc length and are randomly varied using the schematic model. The values assigned to this non-linearity are related to experimental process parameters observed on the workshop. Whilst the range is relatively known but the variation is lesser known, it was decided to consider a random assignment of these values for the SMAW process. When the output was generated with the nonlinear process disturbances, the output for the current and voltage was observed as in Fig. 9 and Fig. 10 respectively.

The waveforms in both the cases show an interesting characteristic behaviour of an inverter power source, where the output current averages to a value in the range of ± 1 A of the set current. This output is also consistent over the period of time of simulation in spite of the random nature of the disturbances. The controlled behaviour of the current indicates that the power source model is capable of replicating the function of an inverter power source. The choice of 130 A is only incidental and the simulation results with other values were seen to be of similar nature thus confirming the ability of the power source to operate in a wider range. Since no fabrication is involved, the range of the output will be limited only to the range of load equation model. The statistical value of the current

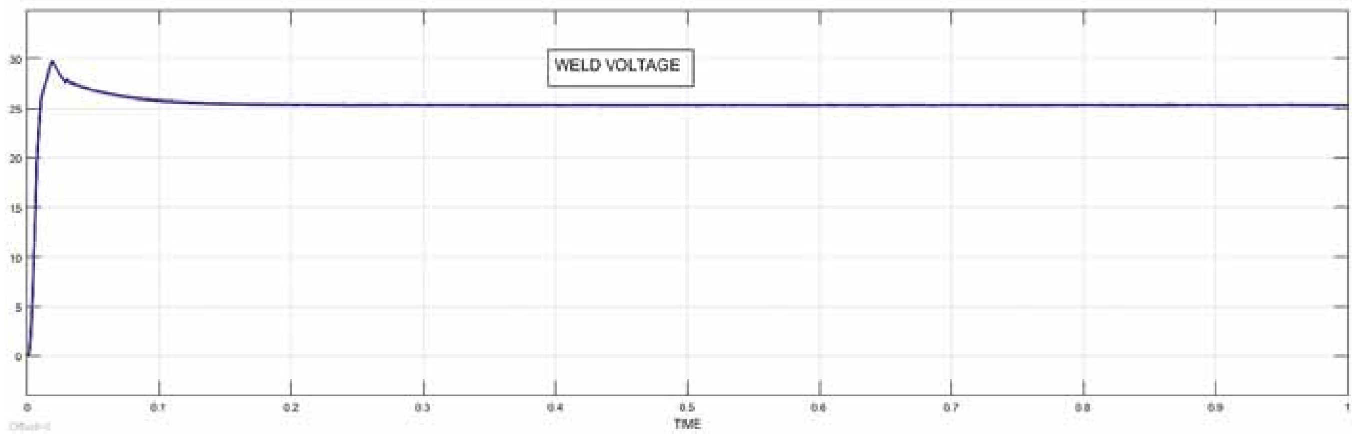

Figure 8 -Voltage output from the power source model with no disturbances

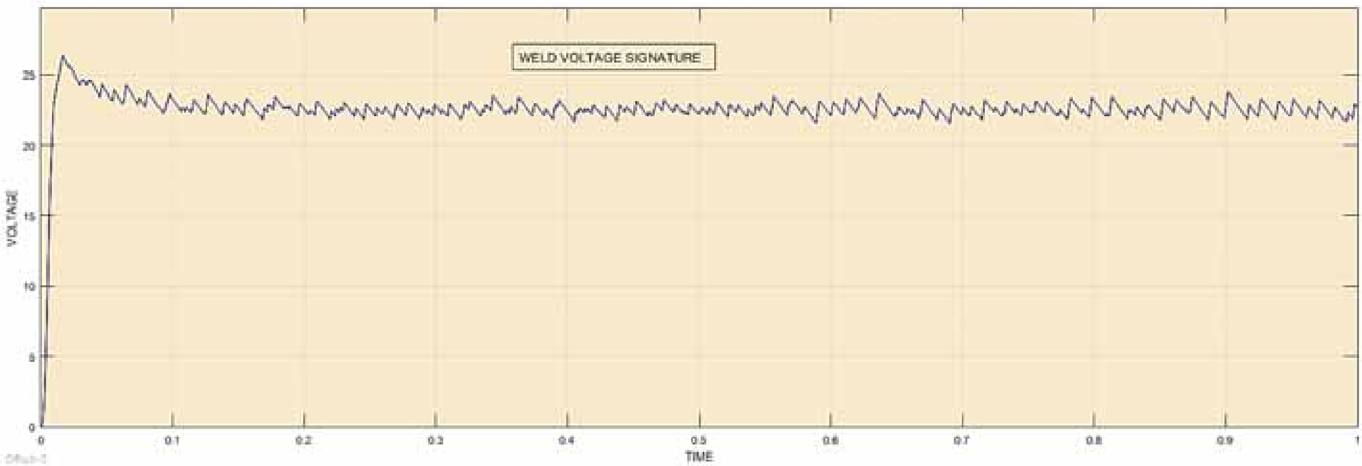

Figure 9 -Voltage output from the power source model with random disturbances

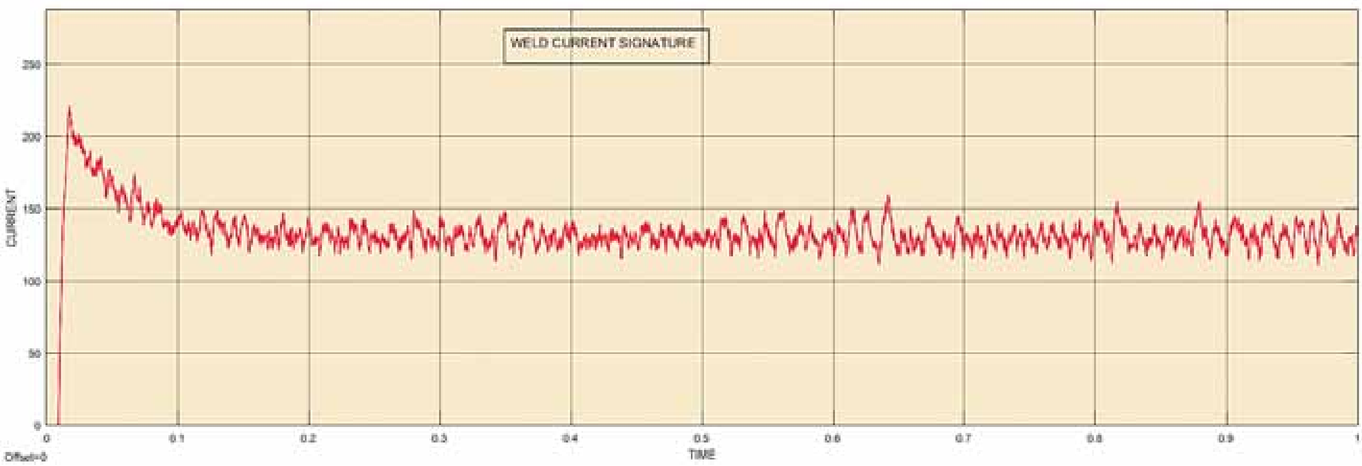

Figure 10 -Current output from the power source model with random disturbances

Table 2 -Statistical average of the output current and voltage

Variable	Set Value	Max	Min	Average
Current	130 A	159.3	110.5	129.22
Voltage	–	23.78	21.58	22.51

and voltage parameters are provided in Table 2. Table 2 establishes that the designed power source model is capable of accepting output current targets that will be delivered in response to the fluctuating environmental operating variables.

6.0 Conclusions

An inverter based power source model has been successfully designed and developed on a Matlab platform and using this model, the output signals which are similar to those from a physical power source have been generated. This model has been successfully employed for the analysis of output signals (current and voltage) in the presence of several process disturbances, which are typically encountered in a welding shop. The good results obtained have validated the model and this model can be employed for the design of future power sources and troubleshoot, wherever necessary.

References:

1. **J. F. Lancaster**, The physics of welding, Pergamon Press, 1986.
2. **Arun Kumar Paul**, Robust Product design using SOSM for control of Shielded Metal Arc Welding Process, IEEE Transactions on Industrial Electronics, Volume: 63, Issue: 6, June 2016, pp. 3717 – 3724.
3. **Killing**, Welding processes and thermal cutting, English Edition, Volume I, DVS Verlag GmbH, 2001.
4. **Pan Jiluan**,Arc welding control, ISBN 1 85573 687 X, CRC Press, 2003.

ICALEO

October 14-18, 2018

Rosen Centre Hotel (Orlando, FL USA)

The International Congress on Applications of Lasers & Electro-Optics (ICALEO®) is viewed as the premier source of technical information in the field.

Laser industry professionals from academic and industrial settings will gather to discuss the latest in laser materials processing, laser micro processing and nano manufacturing. Topics range from the interaction between a laser beam and a material to how a process can be integrated and optimized for an application.

For more details and registration visit www.lia.org

SHEET METAL WELDING CONFERENCE XVIII

Welding solutions for lightweight vehicle production

October 17-18, 2018

Laurel Manor, Livonia, Michigan

The American Welding Society Detroit Section proudly presents the 2018 Sheet Metal Welding Conference, a 3-day event including a welding and joining workshop with demos, a 2-day technical conference and vendor display evening. This event is intended to bring industry experts around the world to interact, present and discuss joining and welding as it pertains to Automotive, Transportation and Light Manufacturing. Please come join us on October 16th, 17th, and 18th for this premier event.

For more details and registration visit www.aws.org

WELDING AND RELATED TECHNOLOGIES – PRESENT AND FUTURE

December 5-6, 2018

Kiev, Ukraine

The International Conference on "Welding and Related Technologies - Present and Future" will be held by the E.O.Paton Electric Welding Institute of the National Academy of Sciences of Ukraine on 5-6 December, 2018 in Kiev.

The invited papers of scientists from different countries of the world about the most important research achievements, obtained during recent years in the field of welding, surfacing, brazing, strength, new materials, NDT and technical diagnostics, evaluation of residual life of welded structures, surface engineering, special electro metallurgy, ecology of welding production, and also about the prospects of progress of these trends will be presented and discussed at the plenary sessions of the conference. Alongside with plenary sessions the poster papers will be also presented.

Main Conference Topics:

- Technology, materials, equipment for welding and related technologies
- Strength of welded structures, theoretical and experimental investigations of stress-strain states and their control.
- Non-destructive testing and technical diagnostics.
- Improvement of welded structures, automation of their designing, evaluation and extension of service life.
- Surface engineering.
- Welding in medicine, technologies, equipment, nano materials and nano technologies.
- Ecological problems in the field of welding production.
- Special electrometallurgy.
- Standardization and certification of products of welding manufacturing, training and attestation of specialists.
- Information technology and welding control systems

For more details and registration visit

http://www.paton100.org/

8TH ASIA PACIFIC IIW INTERNATIONAL CONGRESS March 20-22, 2019

Bangkok, Thailand

The 8th Asia Pacific IIW International Congress has the theme “Promote and Ensure the Quality of Welding Education in the Region”. This is an opportunity for engineers, technicians, lecturers, researchers, educators, suppliers and anyone who are involving in the area of welding technology and joining processes to meet together, learn and share their ideas, information, experiences and acquire the new knowledge in this field.

The large volume of development activity expected for the Asia Pacific in the coming years, more especially on the industrial sectors, constitutes a real challenge for the future for the welding technology, notably in terms of quality education, competitiveness, automation, quality management, and safety.

Main topics:

- Education and training
- Digital transformation of welding industries (Human-robot collaboration, Automated manufacturing, Process control, Inspection, Security, Management, and etc.)
- Construction
- Transportation
- Off-shore oil and gas exploration, production and beneficiation
- Petrochemical and Refinery
- Ship building
- Power generation
- Food & Beverage and Other related research areas

For further details visit

http://iiweling.org/news/8th-asia-pacific-iiw-international-congress

EXPERIMENTAL INVESTIGATION OF LONGITUDINAL BENDING DISTORTION AND WELD SHRINKAGE OF ONE SIDE FILLET WELDED T- JOINTS AND COMPARATIVE ANALYSIS WITH EMPIRICAL FORMULAS

V. Sudharsanam, L. Prakash, M. Madhu and N. Raju

Welding Research Institute, BHEL, Tiruchirappalli-620014

Abstract: *In this article, a detailed investigation of the longitudinal bending distortion of one side fillet welded T joints has been carried out. T joints of various section dimensions, made of IS 1079 HR2 grade of steel sheets were welded using SMAW process. It was observed that, after welding, the T joints bend on account of the weld shrinkage. The distorted weld line took the shape of a parabolic arc. It was further seen that there exists an inverse relationship between welding distortion and the moment of inertia of the cross section and a direct relationship between radius of curvature of weld and moment of inertia of cross section. The experimentally observed values of bending distortion, weld shrinkage and radius of curvature of weld are compared with the respective values obtained using established empirical formulas. The ability of the empirical formulas to closely predict the real time results was assessed and the relative merits and demerits of each of the empirical formula have been discussed.*

Keywords: Longitudinal bending, distortion, T joint, fillet weld, weld shrinkage, curvature of weld

1.0 Introduction

Welding distortion is one of the major bottlenecks in achieving enhanced productivity in structures fabricated by welding. The localized heat liberation associated with a moving arc heat source results in varying levels of heat distribution along the length and breadth of the component being welded. This heterogeneous heat distribution leads to differential levels of subsequent shrinkage in the welded component viz. the points in and very close to the weld line experiences the largest shrinkage strains and the areas farther away from the weld are not affected majorly by the local arc heat. Therefore, this differential levels of heating and cooling causes the welded components to become distorted or warped. There are several types of weld distortions depending on the length of the weld and the types of shrinkage experienced by the weld. The major types include the longitudinal bending distortion, angular distortion, buckling distortion, twist distortion, etc. [1]

Out of the various types of weld distortion, the longitudinal bending distortion is that type of distortion that happens when the length of the weld is quite high and when the weld line is at an offset from the neutral axis of the component. On cooling of the weld, the shrinkage forces that arises in the weld acts with respect to the neutral axis of the component and causes a bending moment. This moment then leads to a bowing type of a distortion, which is referred to as longitudinal bending distortion [1]. This type of distortion is predominantly seen in long welded structures and in long built-up beams like I- beams, T beams, etc.

In this article, the longitudinal bending distortion, longitudinal shrinkage and radius of curvature of weld of long, one-sided fillet welded T-joints have been analyzed and the results have been compared with other established empirical formulae.

2.0 Literature survey

Investigation of welding distortion has been the prime objective of many welding related researches that were conducted towards the later half of the 20th century. One of the foremost and widely acknowledged research in the area of welding distortion was carried out by Okerblom [2]. He has deduced empirical formulas correlating the distortion of a weld to the material properties and the welding process conditions. The Okerblom's formula for prediction of longitudinal bowing deflection (LBD) of a welded structure is given below

$LBD = 0.335 \times (q / v) \times \{\alpha /(C \times \rho)\} \times (Z/I) \times (L^2 / 8)$ .... Eq (1)

Blodgett also proposed an empirical formula for prediction of LBD in steels, based on a multitude of experiments conducted by him [3]. This is presented below

$LBD = 0.04 \times \{(Aw \times Z) / I\} \times (L^2/8)$ .... Eq (2)

Horst Pflug has also put forward a prediction formula for the LBD of welds based on his own experimental results by taking into account the yield strength of the material being welded [4]. This is given below

LBD = {(42 x σy) / E} x {(Aw x Z)/ I} x (L^2/8) ……… Eq (3)

Radaj proposed simple empirical formula for the estimation of longitudinal distortion, derived from the concept of shrinkage force of the weld, using the well-known beam bending equation [5].

LBD = (Fs x Z) x (1/EI) x (L^2/8)……………… Eq(4)

Where, Fs = 10200 x Aw………………… Eq (5)

The symbols used in equations (1), (2), (3) and (4) are explained below

η = Efficiency of welding process (%)
q = Heat flux applied during welding (taken as product of welding current and voltage) (W)
v = Welding speed (mm/sec)
α = Coefficient of thermal expansion (/°C)
C = Specific heat capacity (J/ kg °C)
ρ = Density (Kg/mm^3)
Z = Distance of the weld from neutral axis of the component (mm)
I = Moment of Inertia of the component (mm^4)
L = Length of weld (mm)
Aw = Cross sectional area of weld (mm^2)
σ_y = Yield strength of the base metal (N/mm^2)
Fs = Shrinkage force of the weld (N)
E = Young's Modulus (N/mm^2)

Based on the thermal impulse given to the material during welding, Farkas and Jarmai[6] have also proposed an empirical formula for prediction of welding distortion, which is exactly similar to the formula proposed by Okerblom. FEM based analyses were also conducted by many researchers for prediction of welding distortion and residual stresses. Penso conducted numerical investigations to study bending distortion of a mild steel panel structure [7]. Daniewicz presented a hybrid experimental and numerical approach to predict weld distortion of large ship structures [8]. Michaleris and DeBiccari performed numerical analysis to calculate welding induced distortion in large and complex welded structures [9].

There are several research works that deal with the study of angular distortion of plates forming T joint configuration and connected by fillet welds. Several of these works attempted to predict the welding distortion by numerical simulation [10 - 15]. Some of them have also adopted experimental investigation [16, 17]. However, it is found that there are only a few studies on the longitudinal distortion behavior of long, fillet welded T-joints.

Sasayama initiated a systematic study of longitudinal bending distortion of fillet welded, steel T-joints and correlated them with an apparent shrinkage force, which in turn was dependent on the weight of the electrode consumed per unit length in depositing the weld [18]. On similar lines, Yamamoto performed experiments in Aluminum T-joints and concluded that the shrinkage force of weld could be used for satisfactory prediction of bending distortion [19]. Ravichandran studied the longitudinal bending distortion of steel T joints welded by SAW process using FEM technique and validated the results with experimental observations and found a close match between the two [20].

The present study is aimed at strengthening the understanding of the bending distortion of long fillet welded T-joints, by means of experimentally determining distortion and by comparing the same, with established empirical formulas.

3.0 Experimental Method

T joints of different sizes made of thin sheets of thickness 2.5 mm of structural steel (IS 1079 HR2) were fillet welded in one side of the vertical web plate. The schematic sketch of the T Joint used for the study is shown in Fig. 1 (a). The details concerning the sizes of the T joints and the welding process are presented in Table 1. The mechanical properties of the IS 1079 sheet metal used for the study, as determined by conducting tensile test conforming to ASTM E8 standard are shown in Table 2.

In order to accurately determine the distortion in T joints after welding, the heights of points were measured along the complete length in the top line of the web plate at every interval of 50 mm both prior and after welding. The height measurements were made by placing the T joint in a flat surface and using a calibrated vernier height gauge. The measurement method adopted is shown in Fig. 1(b). The net difference in the measurements made before and after welding is the deflections experienced by the select points present in the top line of the web plate. The maximum deflection was then found out from these measurements and

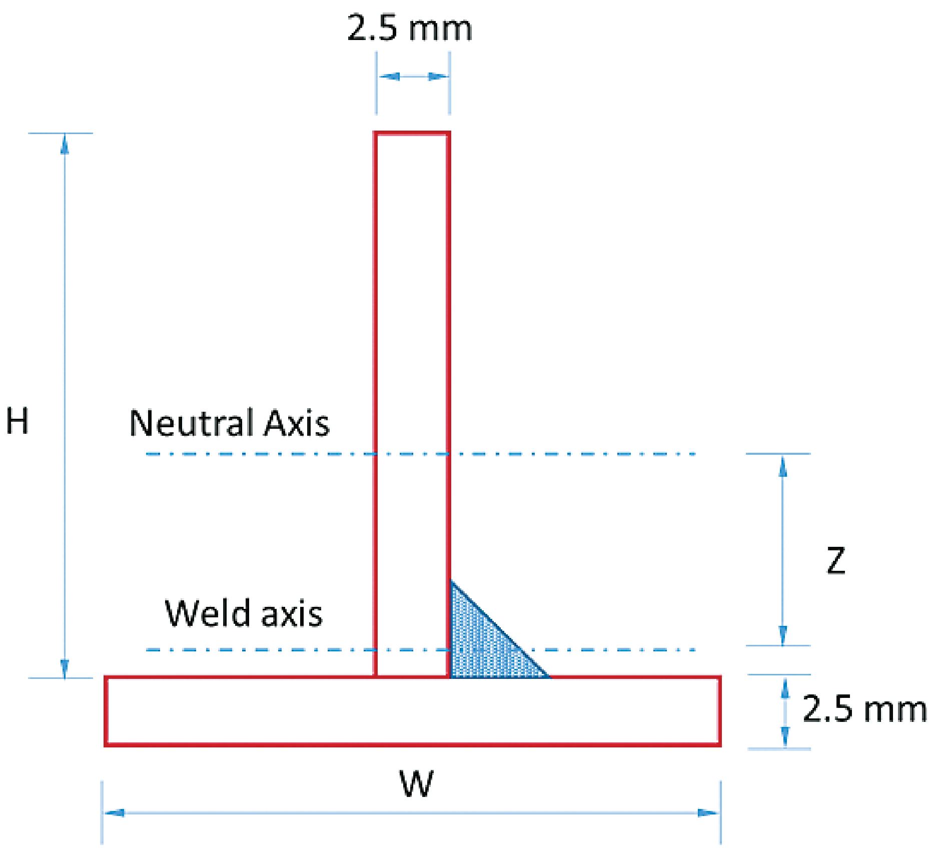

Figure 1 (a) – Schematic sketch of the T joints taken for study

Table 1 – T joint sizes and welding parameters used

Sl. No.	T joint Cross section	T joint Length	Welding parameters					
			Voltage (V)	Current (A)	Welding speed	Electrode class &Size	Process
1	W = 70 mm, H = 50 mm	L = 1200 m	20	70	2.5 mm/sec	E 7018, Ø 2.5 mm	SMAW
2	W = 70 mm, H = 70 mm						
3	W = 70 mm, H = 90 mm						

Table 2 – Mechanical properties of the material used for the study

Material grade	Yield Strength (MPa)	Ultimate Tensile Strength (MPa)	Elongation	Reduction in area
IS 1079 HR2	270	434	44 %	59 %

recorded. The experimentally obtained distortion values were further compared with the predictions made using other established empirical formulas.

Similarly, for measuring the longitudinal shrinkage of the weld, the weld line was measured before welding. After completion of one side fillet weld, the weld line was again measured. However, the measurement of weld line after welding, was not straightforward, as there was a curvature in the weld on account of the longitudinal bending distortion. Hence, a thread was taken and held tightly between one end of the T joint to its other end and it was ensured that the thread exactly traced the profile of the curved weld line. Thereafter, this thread was straightly held and the measurement was again taken. This measurement corresponded to the shrunk length of the weld line. The difference between length of weld line before and after welding yielded the longitudinal shrinkage of the weld, in each variants of the T

Figure 1(b) – Method of measurement of distortion of the top line of the web plate using a vernier height gauge

joints. The measurements were taken by using a measuring scale and a vernier caliper. The experimentally obtained shrinkage values were further compared with the predictions made using established empirical formulas.

Besides the bending distortion and longitudinal shrinkage of weld, the radius of curvature of the weld line after welding was also calculated. The deflection measurements of points present in the top line of the web plate, at an interval of 50 mm spacing, were plotted as coordinate points in a graph and the points were fitted into a curve of best fit. Then, the radius of curvature of the curve in the centre of the length of weld was calculated using the following equation

$R = [\{1 + (Y'(x))^2\}^{3/2}] / Y''(x)$ .... Equation (6)

Where, Y (x) is the equation of curve of best fit, representing the top line of the distorted web plate

Y'(x) represents the first derivative and Y''(x) represents the second derivative.

After obtaining this radius, height of the web plate was subtracted in order to arrive at the radius of curvature of the weld line. This radius of curvature so obtained was compared with that obtained using the established empirical formulas.

4.0 Results and Discussion

It was found that, in each of the T joints, a longitudinal bow was noticed and the extent of bow varied with respect to the sectional dimensions of the T joint. It is observed that the end of web plate connected to the flange plate decreased in length on account of the weld shrinkage and the other end of the web plate which is parallel to this end experienced an increase in length. Since the weld axis is separated from the neutral axis by a considerable distance in each of the T joints, the shrinkage forces arising during the cooling phase of the weld results in the creation of a moment that leads to longitudinal bending of the T joints. This is shown in Fig.1(c).

4.1 Longitudinal bending distortion

Theoretical calculations of distortion were carried out as per the equations (1), (2), (3) and (4) mentioned earlier. The values for the terms in these equations are presented in Table 3(a) and the calculations are given in Table 3(b). The experimentally observed distortion results alongside the predictions made using the empirical formula put forward by Okerblom, Blodgett and Horst Pflugare presented in Table 4.

It is observed from Table 4, that as moment of inertia of the T joint increases, the bending distortion decreases confirming the inverse relationship inferred from equations (1) to (4). A bar chart of the values of weld distortion observed experimentally and those calculated using formulas deduced by Okerblom, Blodgett, Horst Pflug and Radaj for each size of the T joints is shown in Fig. 2.

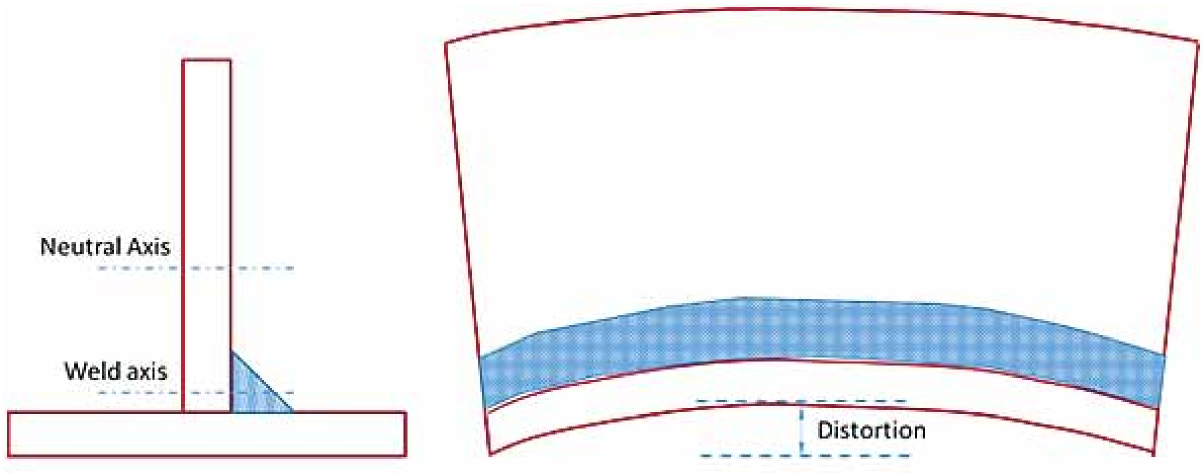

Figure 1(c) – Distorted shape of T joint after welding due to weld shrinkage

Table 3(a) –Values taken for symbols used in equations (1), (2), (3) and (4)

Symbol	Values taken for computation
	Assumed as 0.65 (for SMAW process)
q	Product of V & I (in watts) (taken from Table 1)
v	2.5 mm/sec
α	1.1 X 10^{-5}(/° C)
C	510j/ kg ° C
ρ	7.850 X 10^{-6}Kg/mm^3
Z	Referred from Table 2(b)
I	Referred from Table 2(b)
L	1200 mm
Aw	½ x $(\text{leg size})^2$ = ½ x $(3)^2$ = 4.5 mm^2,(leg size: 3 mm)
σy	270 MPa (from Table 2)
E	210000 MPa

By refer ring to Fig. 2, it could be inferred that Okerblom's formula over estimates the distortion by an average magnitude of +25%. The positive error indicates that predicted value is always higher than the experimentally observed one. The reason for this error could be attributed to minor errors associated with the assumption of arc efficiency and in the estimation of heat input, as the welds were made by SMAW process which was done manually.

The Blodgett's formula estimates the distortion by an average magnitude of -32.7% error. The negative error indicates that this formula has resulted in the underestimation of magnitude of distortion compared to the experimentally observed value. The reasons for this error level could be attributed to the precise estimation of area of the fillet weld which could have had some variations along the length, as the weld has been deposited manually.

Table 3(b) – Calculation of Moment of Inertia and distance between weld axis and neutral axis

(1) Calculation of Moment of Inertia

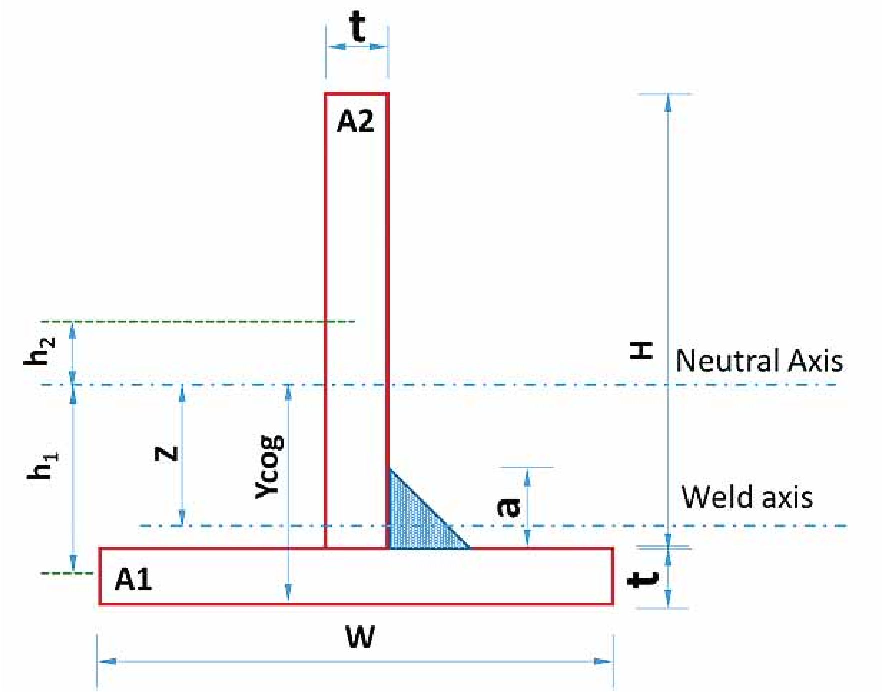

Figure 1 (d) – T joint with representation of various dimensions

Moment of Interia of T section, I = $[\{(W*t^3)/12\} + (A1*h1^2)] + [\{(t*H^3)/12\} + (A2*h2^2)]$

The notations used in the above equation are listed below in reference to figure 1(d)
t = thickness of web plate = thickness of flange plate = 2.5 mm

W = width of bottom flange plate (mm)

H = Height of web plate (mm)

A1 = Area of flange plate = (W*t) (mm^2)

h1 = distance of separation between midline of flange plate and neutral axis of the T section (mm)

A2 = Area of web plate = (H*t) (mm^2)

h2 = distance of separation of midline of web plate from neutral axis of the T section (mm)

(2) Calculation of offset distance of weld axis from neutral axis

Z = Ycog – t – (a/3)
Where,
Ycog = Distance of separation of the neutral axis of the T section from base line of flange plate = $\{(Wt^2)+(tH^2)\}/2(A1 + A2)$ (expressed in mm)

A1 = (W*t) (mm^2)
A2 = (H*t) (mm^2)

Z = Offset distance of the weld axis from the neutral axis of the T section (mm)
a = leg length of fillet weld = 3 mm

Table 4–Weld distortion observed experimentally and obtained using empirical formulas

T joint Size (W x H) (mm)	I (mm^4)	Z (mm)	Distortion values								
			Experi mental (mm)	Okerblom		Blodgett		Horst Pflug		Radaj	
				Predict ion (mm)	% Error	Predict ion (mm)	% Error	Predict ion (mm)	% Error	Predict ion (mm)	% Error
70 x 50	76377	8.70	5.06	6.87	35.77	3.69	-27.07	4.98	-1.58	4.48	-11.46
70 x 70	186530	15.62	4.40	5.05	14.77	2.71	-38.40	3.66	-16.81	3.30	-25.00
70 x 90	363000	23.77	3.15	3.95	25.40	2.12	-32.70	2.86	-9.20	2.58	-18.09
Average error in estimation					25.31		-32.72		-9.1		-18.18

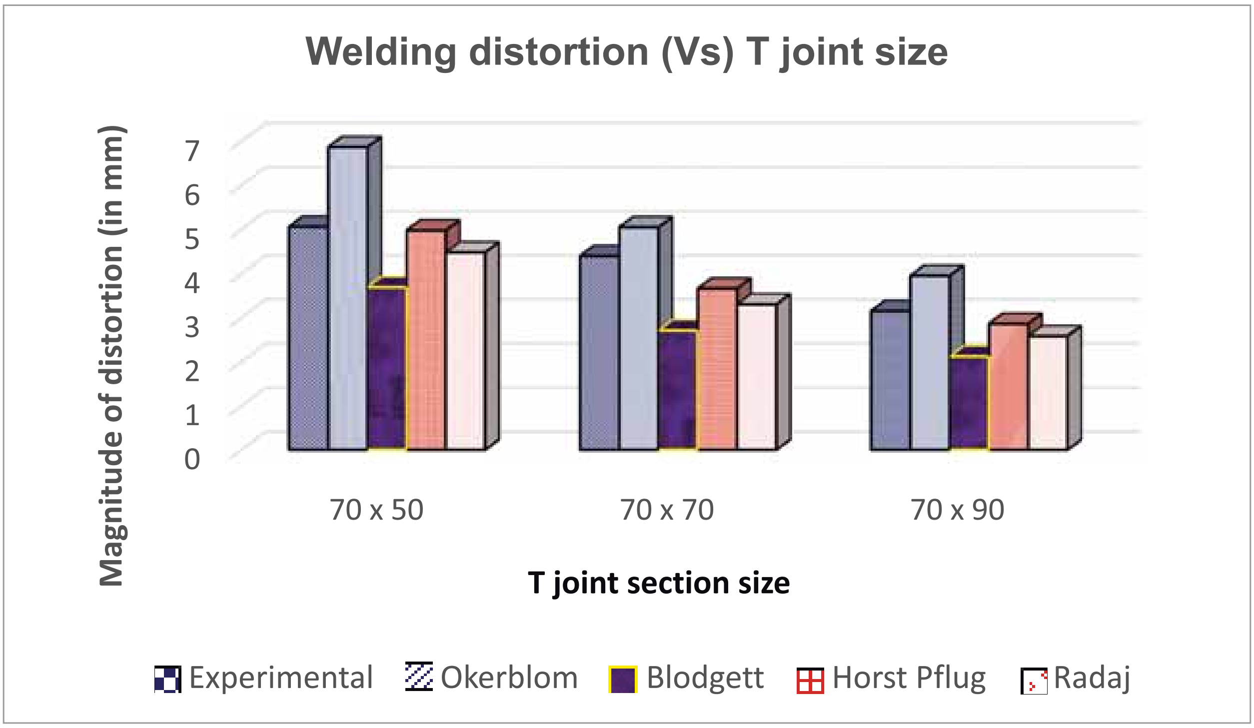

Figure 2 –Bar chart showing experimental and predicted values of longitudinal bending distortion

The distortion values predicted using the Horst Pflug's formula has resulted in good match with that seen experimentally. The maximum error observed in this case is 16.8% and the average error considering the three cases of T joints is within 10% of the experimentally observed value. The reason for this could be the errors originating in precisely estimating the yield strength and area of weld. The former factor could be affected by sheet metal anisotropy and the latter factor could be due to variations in weld size along the length of the weld.

The Radaj's formula has also resulted in underestimation of distortion. The average error in the estimation of the distortion comes to around -18.1%, which seems to be reasonable. The reason for the error could be due to the error caused in the computation of the shrinkage force of weld, calculated from the empirical relationship presented in equation (5). The degree of accuracy of this formula could largely influence the values estimated using the equation (4). Therefore, if we had other means to compute the weld shrinkage force precisely, perhaps, this formula might have resulted in a prediction of weld distortion, with a higher accuracy.

Thus, from the foregoing discussions, it could be inferred that Horst Pflug's formula predicts the distortion value to a much closer extent than any of the remaining three formulas. This is so because the average error level in prediction is observed to the least (-9.1%) among all the formulas analyzed. The second best estimate is provided by the Radaj'sfomula, which is found to show an average error level of around -18% compared to the experimental values. The Okerblom's formula is found to be the next best estimate with an observed average error level of +25% in predicted values of distortion in comparison to the real time values. The Blodgett's formula is found to yield predictions of distortion with an average error level of -32%, the highest among all the four empirical formulas discussed herein. It is also further seen that, while Okerblom's formula results in over estimation of magnitude of bending distortion, the remaining three namely Horst Pflug's formula, Blodgett's formula and Radaj's fomula have all resulted in underestimation of magnitude of bending distortion. However, it can be seen that all the formulas have resulted in reasonably good predictions of the magnitude of bending distortion of one side fillet welded T joints.

4.2 Longitudinal shrinkage of weld

The weld shrinkage is primarily responsible for the longitudinal bowing distortion. The magnitudes of shrinkage of the welds in each of the T joints are presented in Table 5. Besides this, the predicted value of weld shrinkage is also listed in Table 5. These predictions have been made by making use of the following equations

$\delta L = 5175 \times (Aw \times L)/(A \times E)$……… Equation (7)

$\delta L = 6720 \times (Aw \times L)/(A \times E)$……… Equation (8)

$\delta L = (Fs \times L) / (A \times E)$……… Equation (9)

Where,

δL = Longitudinal shrinkage of fillet weld (mm)

A = Cross sectional area of the T joint (mm^2)

Fs is defined as in equation (5)

The formula specified in equation (7) has been deduced by Guyot et al [4] and the formula specified in equation (8) has been put forward by Mamlin[4]. The equation (9) above is Radaj's formula for prediction of longitudinal shrinkage of weld [5]. The comparative presentation of the experimentally observed shrinkage of welds in each of the T joint and those values predicted using the equations (7), (8) & (9) mentioned above, are shown in the bar chart in Fig. 3.

Referring to Fig. 3 and Table 5, it is observed that as the moment of inertia of the T joint increases, the shrinkage of the weld decreases. This is also concurrently happening with the reducing trend in the distortion values also, as observed in Table 2. Thus, with the increase in moment of inertia of the T joint, both the shrinkage and bending distortion exhibits a reducing trend. This is so because, as the section's moment of inertia increases, the structure becomes more rigid thereby making it very hard to bend.

Further, as far as the prediction accuracies are concerned, it is found that the average error in prediction of longitudinal shrinkage of weld, based on Radaj's formula comes to 0.95% only. Further, the maximum error level is approximately 13% and this is observed as both positive magnitude and negative magnitude. Nevertheless, this formula can be understood to predict longitudinal shrinkage of fillet welded T joints very closely. The remaining two formulas proposed by Guyot et al and Mamlin grossly under estimates the longitudinal shrinkage and does not

Table 5 – Comparative presentation of weld shrinkage observed experimentally and obtained using empirical formulas

T joint Size (W x H) (mm)	Moment of Inertia	Shrinkage values (in mm)						
		Experimental Value	Guyot et al		Mamlin		Radaj	
			Prediction	% Error	Prediction	% Error	Prediction	% Error
70 x 50	76377	2.0	0.44	-79.04	0.57	-72.85	1.81	-13.80
70 x 70	186530	1.4	0.38	-74.66	0.49	-67.33	1.55	3.33
70 x 90	363000	1.2	0.33	-72.50	0.43	-64.16	1.36	13.33
Average error in estimation				-75.40		-68.11		0.95

exhibit any closeness to the experimentally observed shrinkage values. Therefore, it is understood that these two formulas do not predict the longitudinal shrinkage of fillet welded T joints accurately. The reason could be due to the simplifying assumptions the authors might have taken, while deducing these formulas.

4.3 Radius of curvature of weld

It is observed that the bowing distortion of the T joint resulted in the formation of a curvature of the weld line. The profile of the top line of the distorted web plate of each of the T joint is graphically presented in Fig. 4, 5 and 6. In each of these figures, the curve of best fit is drawn using dotted lines. It is seen that the curve of best fit happens to be a parabola. This is in agreement with the empirical equations (1), (2), (3) and (4). It is evident from these equations that distortion is directly proportional to square of length of the weld. Therefore, it is understood that when all other factors of equations (1) to (4) are kept constant and if we vary the length alone, we obtain deflections that are proportional to the square of length of the weld. Thus, we end up with a distorted shape of the weld that is parabolic in nature.

The general equation representing these parabolic curves is given below

$Y = AX^2 + BX + C$ .... Equation (10)

The values of 'A', 'B' and 'C' for each of the distorted T joint are presented in Table 6. These were computed using curve fitting options available in *Origin graphing software*. The radius of curvature for each of the parabolic curve representing the distorted shape of the top line of the web plate of each T joints were calculated using equation (6). The radius of curvature values so computed are presented in Table 6. In order to obtain the actual radius of curvature of the weld line, the above values were then subtracted by the web plate height. These values are also presented in Table 6.

Having obtained the actual radius of curvature of weld, this quantity is compared with that predicted using the empirical equations (1) to (4). Each of the equations (1) to (4) can be rewritten in the following general form

$LBD = (1/R) \times L^2/8$ .... Equation (11)

Where R = Radius of curvature of weld (in mm)

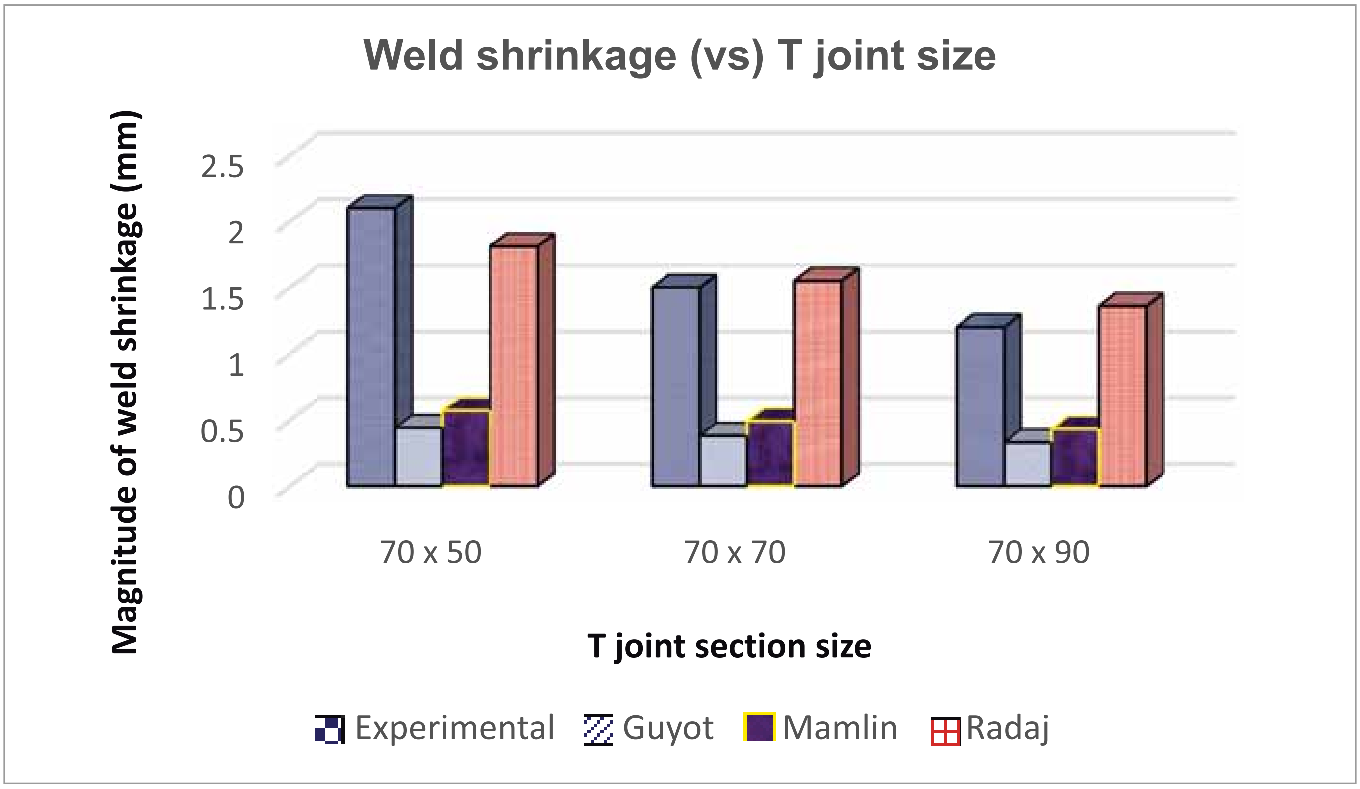

Figure 3 – Bar chart showing experimental and predicted values of weld shrinkage

Referring to equation (11), the radius of curvature of weld of each of the distorted T joint is computed using each of the four empirical formulas (equations (1) to (4)). These values are presented in Table 7. Together with these values, the radius of curvature of weld deduced from the experiments is also presented in Table 7. Further, the comparative presentation of the predicted radii of curvature and those obtained experimentally, is made in the bar chart shown in Fig. 7.

Referring to Table 7 and Fig.7, it is inferred that as the moment of inertia of the section increases, the radius of curvature also increases. Further, it is seen that the Okerblom's formula underestimates the radius of curvature of weld in each of the T joint with the average error in prediction standing at -16.98%. This is in keeping with the earlier observation that the same formula resulted in over estimation of weld distortion. The Blodgett's

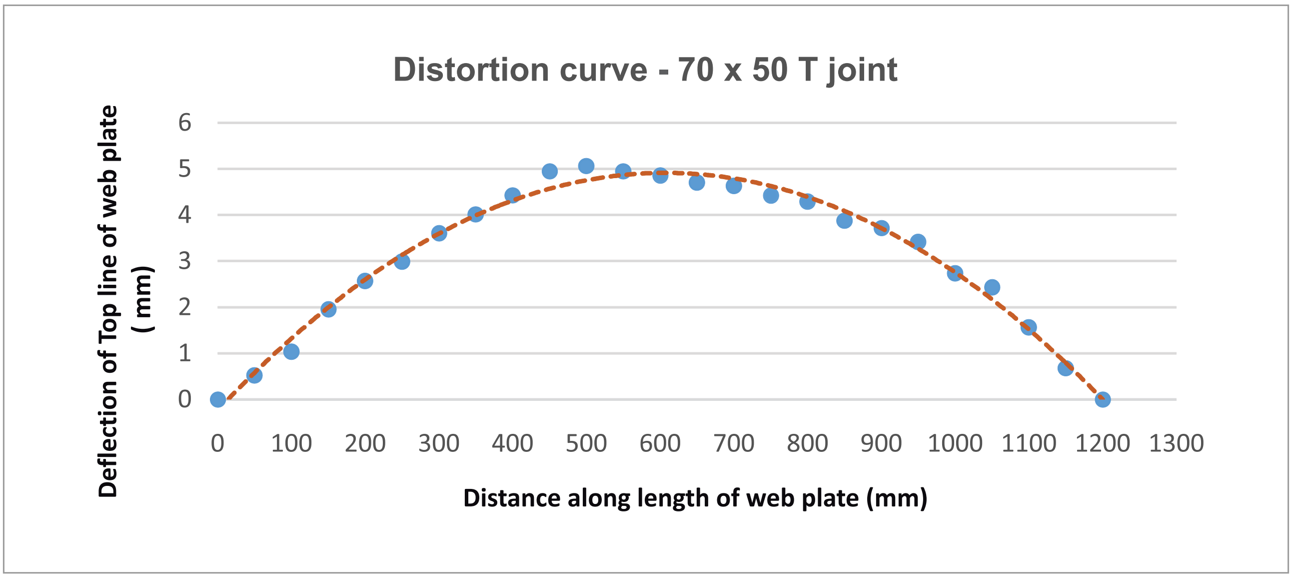

Figure 4 – Distorted shape of the top line (un-welded edge) of web plate of (70 x 50) T joint

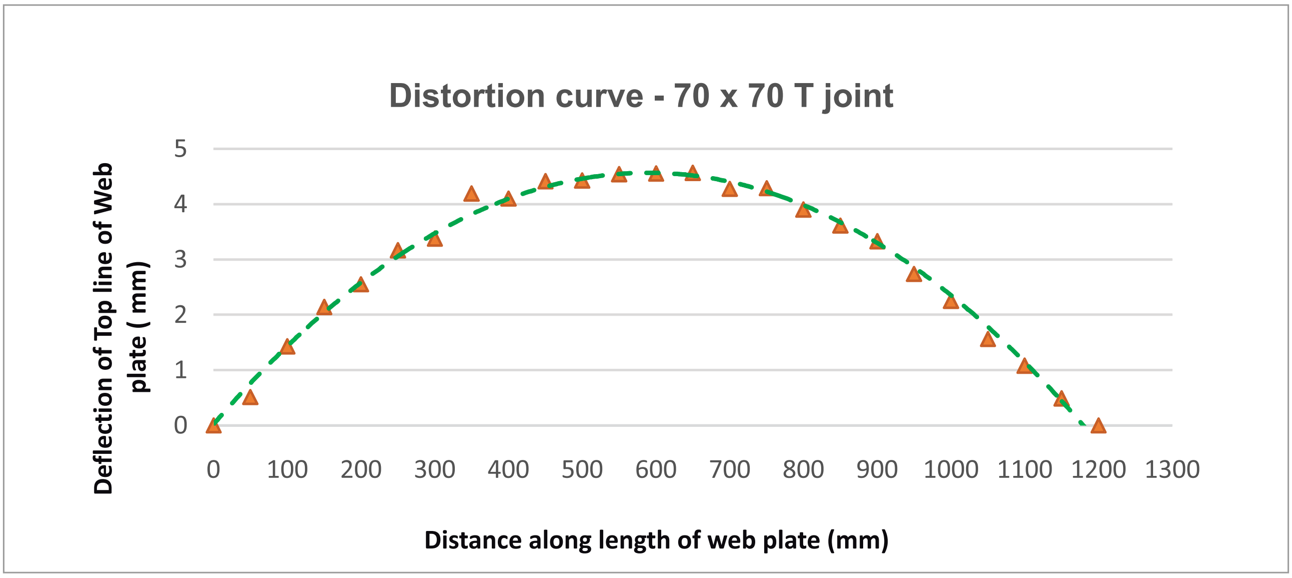

Figure 5 – Distorted shape of the top line (un-welded edge) of web plate of (70 x 70) T joint

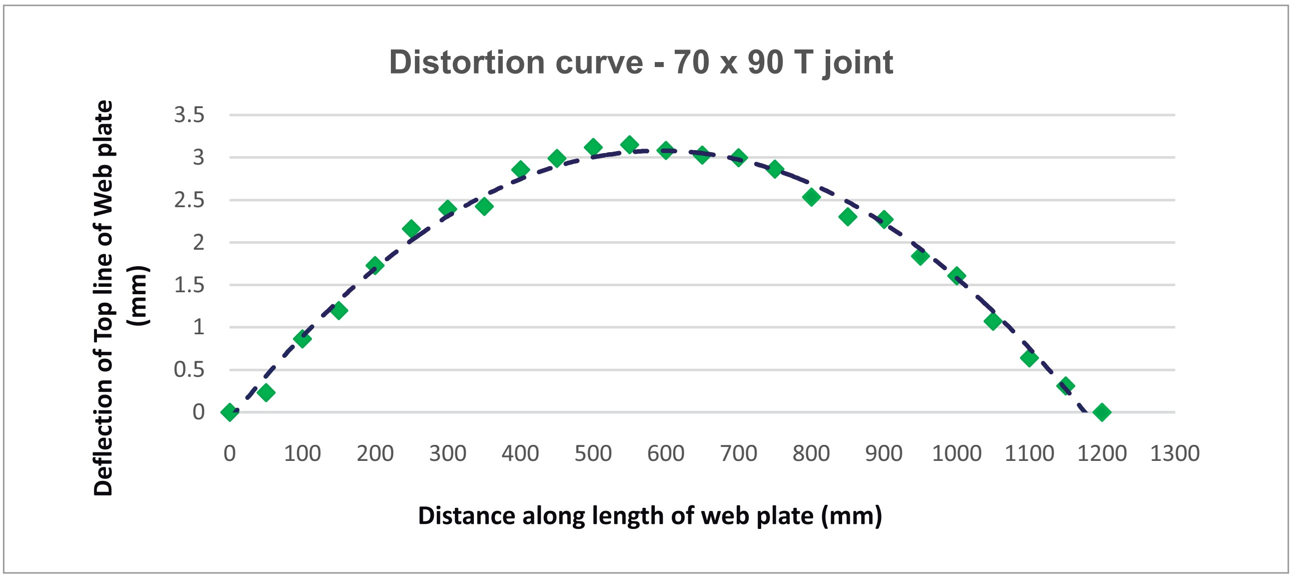

Figure 6 – Distorted shape of the top line (un-welded edge) of web plate of (70 x 90) T joint

Table 6– Computed values of radii of curvature of weld for each of the T joints

T joint	A (x 10^{-5})	B (x 10^{-5})	C (x 10^{-5})	|Y'(x = 600)| (x 10^{-4}) *(at middle of weld)*	|Y''(x = 600)| (x 10^{-5}) *(at middle of weld)*	Curvature (x 10^{-5}) mm^{-1}	Radius of Curvature of curve (in mm)	Radius of Curvature of weld (in mm)
70 x 50	-1.396	1.6943	-23.117	1.91	2.79	2.79	35816	35766
70 x 70	1.3095	1.5423	2.0957	2.57	2.62	2.62	38182	38112
70 x 90	-0.9014	1.0676	8.3897	1.41	1.8	1.8	55466	55376

formula, Horst Pflug's formula and Radaj's formula have resulted in over estimation of the radius of curvature of weld by average error margins of 54.52%, 14.58% and 27.15% respectively. It may be pertinent to note that these three formulas had earlier resulted in under estimation of weld distortion. This confirms that there exists an inverse relationship between weld distortion and radius of curvature of weld.

5.0 Conclusion

T joints with varying sectional dimensions were subjected to one side fillet welding. The post-weld bending distortion, longitudinal shrinkage of weld and radius of curvature of the weld were experimentally determined and these quantities were compared with those predicted through certain empirical formulas. The experimental and the predicted values were compared. The following conclusions are drawn from the above study.

- The fillet welding of T joints leads to a longitudinal bending distortion, wherein the weld line distorts and attains the shape of an arc segment of a parabola, befitting the various empirical formulas.
- As moment of inertia of the welded T joint increases, the bending resistance of the joint increases and this results in a decreasing trend in the longitudinal bending distortion. This is further accompanied by a decreasing trend in longitudinal shrinkage of weld and in an increasing trend in the radius of curvature of weld.
- The Okerblom's formula results in a minor overestimation of bending distortion and consequently in an under estimation of radius of curvature of weld. The Horst pflug's formula and Radaj's formula result in slight underestimation of bending distortion and overestimation of radius of curvature of weld.

Table 7 –Comparative presentation of radius of curvature of weld observed experimentally and obtained using empirical formulas

T joint Size (W x H) (mm)	Moment of Inertia (mm^4)	Distortion values								
		Experimental (mm)	Okerblom		Blodgett		Horst Pflug		Radaj	
			Prediction (mm)	% Error	Prediction (mm)	% Error	Prediction (mm)	% Error	Prediction (mm)	% Error
70 x 50	76377	35766	26202	-26.74	48772	36.36	36144	1.05	40178	12.33
70 x 70	186530	38112	35631	-6.5	66321	74.01	49180	29.04	54545	43.11
70 x 90	363000	55376	45580	-17.69	84840	53.20	62937	13.65	69767	26.00
Average error in estimation				-16.98		54.52		14.58		27.15

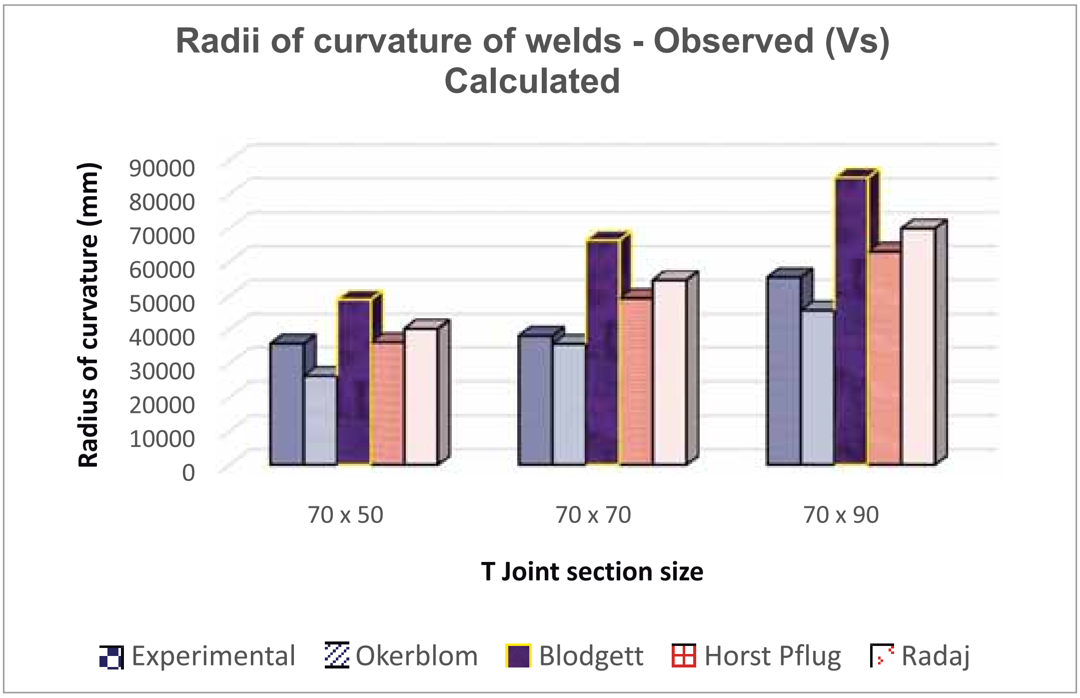

Figure 7 - Bar chart showing experimental and predicted values of radii of curvature of welds

- The Blodgett's formula results in under estimation of bending distortion and over estimation of radius of curvature of weld by a relatively higher level of average error when compared to the remaining three empirical formulas.
- All the four empirical formulas have resulted in reasonably good predictions of bending distortion of weld.
- The Radaj's formula predicts the longitudinal weld shrinkage within a maximum error level of 13% thereby making it a good choice for prediction of longitudinal shrinkage of weld. Both the Guyot's formula and the Mamlin's formula result in poor predictions of longitudinal shrinkage of weld.

References

1. References from World Wide Web: http://www.twi-global.com/technical-knowledge/job-knowledge/distortion-types-and-causes-033/
2. **Okerblom, N.O**, The calculation of deformations of welded metal structures, HMSO, London, UK, 1958
3. **Blodgett,O.W.**, Design of weld structures, published by James. F. Lincoln Arc Welding Foundation, USA, 1982, pp. 7.7-1 to 7.7-10.
4. **Verhaeghe,G**, Predictive formula for weld distortion - a critical review, Industrial Members Report No. 641, The Welding Institute, U.K., 1998.

5. **Radaj, D**, Heat effect of welding – Temperature field, Residual stress, Distortion, Published by Springer – Verlag – USA, 1992.

6. **Farkas J and Jármai K**, Analysis of some methods for reducing residual beam curvatures due to weld shrinkage, Welding in the World, 1998, 41 (4), 385-398.

7. **Penso, J. A**, Development of a PC based FEM model to predict weld distortion, Master's thesis. The Ohio State University, Columbus, Ohio, 1998,.

8. **Daniewicz, S. R, McAninch, M. D, McFarland, B, and Knoll, D**, Application of distortion control technology during fabrication of large offshore structures". Proc. of AWS/ORNL International Conference on Modelling and Control of Joining Processes, 1993.

9. **Michaleris, P, and DeBiccari, A**, Prediction of welding distortion, Welding Journal 76(4), 1997, pg. 172-s to 179-s.

10. **Mikami, Y, Mochizuki, M, Toyoda, M,andMorikage, Y**, Measurement and numerical simulation of angular distortion of fillet welded T-joints – Welding angular distortion control by transformation expansion of weld metals (Report 1) – Welding International, 21:8, 2007, 547-560

11. **Jung, G**, Plasticity-based distortion analysis for fillet welded thin plate T-joints, Ph.D. thesis, Ohio State University, Ohio, USA. 2003

12. **Tso-Liang Teng, Chin-Ping Fung, Peng-Hsiang Chang, Wei-Chun Yang**, Analysis of residual stresses and distortions in T-joint fillet welds, International Journal of Pressure Vessels and Piping, Volume 78, Issue 8, 2001.

13. **MatoPerić, ZdenkoTonković, Alan Rodić, Martin Surjak, Ivica Garašić, Ivanka Boras, SrećkoŠvaić**, Numerical analysis and experimental investigation of welding residual stresses and distortions in a T-joint fillet weld, Materials & Design, Vol. 53, 2014

14. **Adak M and Soares CG**, Residual Deflections and Stresses in a Thick T-Joint Plate Structure, Journal of Applied Mechanical Engineering, 2006, Vol. 5 (6).

15. **Guangming Fu, Marcelo Igor Lourenço, MenglanDuan, Segen F. Estefen**, Influence of the welding sequence on residual stress and distortion of fillet welded structures, Marine Structures, Volume 46, 2016, Pages 30-55.

16. **Jayaraman N**, Predicting angular distortion in arc welding, Ph.D Thesis, Bharathiar University, Coimbatore, India, June 2000.

17. **La Porta Neto, Dante Gageiro, Gonzalez, Arnaldo Ruben, &Mazzaferro, José AntônioEsmerio**, Analysis of the influence of tab thickness, core thickness and welding energy on angle distortions in fillet angle,Welding & Inspection, 22 (2), 2017, 174-193.

18. **Sasayama T, Masubuchi, K, and Moriguchi S**, Longitudinal deformation of a long Beam due to fillet welding," Welding Journal, 34 (12), 1955, pp. 581-s to 582-s.

19. **YamamotoC**, "Study of longitudinal distortion of welded beam," M.S Thesis, Massachusetts Institute of Technology, U.S.A, May 1975.

20. **RavichandranG**, Analysis of transient deflections in welded T beam structures, M.S Thesis, IIT Madras, Chennai, 1987


in Association with
Messe Düsseldorf India
DVS
WRI
MESSE ESSEN
AWF
Concurrent with
WELDING & CUTTING
INDIA
IWS
Cordially Invites you for the
International
WELDING Symposium
IWS 2k18
Theme
Joining, Evaluation and Training - Trends
(JET Trends)
NOVEMBER 27 – 29, 2018
Bombay Convention & Exhibition Centre
(BCEC) GOREGAON (E)
Mumbai, India
For Details Contact:
N RAJASEKARAN
Organising Secretary (IWS 2k18)
Indian Welding Society
Institutions Building, Near 'B' Sector Shopping Centre,
Kailasapuram, BHEL, Tiruchirappalli – 620 014, India
Phone: +91 431 2572988/2702/2551847
E mail: iwsindiaevents@gmail.com /
hqiwsindia@gmail.com
Websites: www.iws.org.in / www.iwsevents.com

Authors are invited to make presentations in the Symposium and can send the abstracts in the following areas.:

- Power & Energy
- Structural fabrication
- Pressure vessels, tanks and high temperature applications
- Ship building
- Aero space
- Automobile and Surface transportation
- Non ferrous materials
- Process industries
- Industry 4.0
- Robotics & Automation
- Additive Manufacturing
- Process and Power Source developments
- Consumables
- Repair & Reclamation
- Surfacing
- Heat treatment methods
- Welding Metallurgy
- Modelling & Simulation
- NDE & its Advances
- Safety and environmental issues
- Skilling & Qualification
- QA & QC in Welding

Delegate Fee has to be paid by presenting author on receipt of acceptance of abstract from Technical Committee of IWS 2k18

GMAW PROCESS FOR ENHANCED ROOT PENETRATION FOR HEADER TO STUB WELDING APPLICATIONS

A.Santhakumari[a], T. Senthilkumar[b], D.K. Verma[a] and Lucky Gaur[a]

a-Welding Research Institute, BHEL, Tiruchirappalli - 620014
b-Anna University, Tiruchirapalli

Abstract: *Headers are very critical products in a power boiler. They essentially take care of the distribution of the steam through various tubular circuits in the boiler. The headers essentially consist of thick walled pipes of diameters upto 960 mm, and thicknesses of even 120 mm. Holes are drilled on the pipe to which stubs are welded. The stubs in turn will get welded to the heat transfer coils. The number of such stubs could be as much as 1200. The integrity of the header to stub weld is of prime importance to prevent any leakage at site. It is also very difficult to repair the leaks, if any, at sites considering the space constraints in an erected boiler. The header to stub welds are done by Shielded Metal Arc Welding (SMAW); and has not been easily amenable for any robotics or automation, considering the close pitching of stubs and also because of lengthy stubs with bends. Welding Research Institute (WRI) has been working with many of the new generation waveform controlled Gas Metal Arc Welding (GMAW) power sources. WRI carried out extensive trials and examined the root penetration and repeatability for header to stub joints using a waveform controlled GMAW process and found to be successful. Based on the success, the technology has been attempted on actual header fabricated in shop floor and hydro tested successfully.*

Keywords: GMAW, waveform controlled power sources, header to stub welding, hydro test

1.0 Introduction

For welding stubs of thickness ranging from 5 – 10 mm and of diameter varying from 58 – 63 mm size to header pipe, SMAW process (Fig.1) is usually employed. With multi pass SMAW to complete the stubs on pipe, a lot of care has to be exercised to avoid defects like slag inclusion, porosity, etc. which can lead to issues like low rate of production, rework during fabrication, repair of shop hydro leaky joints, etc. Further, leakage during hydro test at site affects the project schedules and hence, in the shop, 100% hydro test has to be carried out for all the headers after fabrication. Also, headers with assembled stubs may get strained during transportation, improper handling or erection (overloading) resulting into failures taking place at various stages until being put to operation. This requires excess lengths to be given for stubs, plug welds to be made on all the stubs, and later after hydro test, trimming the excess length of stubs which is time consuming and cumbersome procedure.

Figure 1 - Manual welding of Header to stub

In the current practice of welding of stubs to header, the operation sequence involves bevelling and weld preparation of stubs (Fig. 2), tack welding of stubs to the main body, welding stubs with the header by SMAW process with minimum two different sizes of electrodes for root and filler passes, hydro testing at hydraulic pressures varying from 60 to 300 bar, as required. Welding of stubs to header by SMAW process, apart from low arcing time, consumes more time for slag removal, grinding and cleaning. Moreover, care should be taken while welding of first layer, as it may lead to fusion related problems due to restricted access. Also, due to its typical joint design (set on joint), root is not accessible to penetrate, which can lead to leakage at site during hydro test. Since, the geometry of the stubs is not straight and has more length, they are not conducive for easy automation.

Figure.2 - Edge preparation on header pipe and stub & Stub with complete root pass

1.1 Waveform Controlled Power Sources

A traditional power source uses a transformer to turn high voltage, low amperage primary power into low voltage, high amperage power required for welding. An inverter power source, takes input power, filters it to DC and using fast solid-state switches, increases its frequency to 20,000 to 100,000 Hz. Then, it transforms the current into useable welding power through an advanced level of control over the arc. The intense research and development resulted in the development of the unique concept of Waveform Control Technology™ which has the ability to customize waveform output. With these digital power sources, several improvements were accomplished besides better process control and reproducibility. These modern power sources blend the advances in power electronics and sophistication of high speed computing with the power of inverter technology to generate the desired welding current and voltage parameters.

For the current application of header to stub joints, the use of conventional GMAW process in short circuit mode, which is operated at relatively low voltages and amperage ranges can cause issues related to penetration and fusion. Hence, the use of spray transfer shall be required but the amperage requirement will be high (Fig. 3).

Developments in modern microelectronics have led to rapid advances in welding power sources. With the use of fast microelectronic circuits, the speed of welding process control and welding parameter adjustment has increased tremendously, and

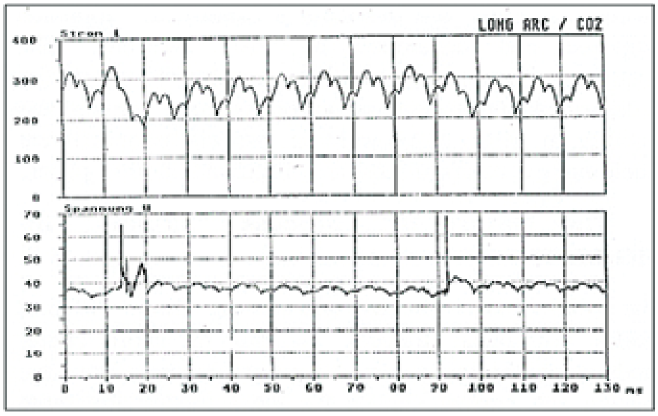

Figure.3 - Current and voltage waveform of spray transfer

dynamic control over arc and molten metal transfer has become possible. With modern digital control power sources, it became possible to intervene the process at a rapid control speed with a very short arc and longer short-circuit phases. This technique could be a choice for achieving deep penetration joints, which is required especially for header to stub joints that is being discussed. This development can offer advantages like improved weld quality, productivity as well as reduced process time.

2.0 Experimental trials and testing

The header to stub welding has been tried with waveform controlled Force Arc semi-automatic GMAW process in the deep penetration mode. Initially, bead on plate (BOP) welding trials were carried out with different contact tip to welding distance (CTWD) to study the variations in penetration. Trials have been done on plate for CTWD from 20 mm to 35 mm and it was observed that the penetration achieved by all these trials were same (Fig. 4).

2.1 Header to stub welding

The experience gained in BOP welding trials have been used to carry out the welding of mock up header to stub joints with the force arc GMAW power source. T22 stubs of different diameter and thickness were welded to a mock up header made of P12 material. The root pass welding had been carried out with stick out length of 20 to 25 mm and wire feed speed of 10.2 – 10.7 m/ min. The shield gas comprising of 85% Argon + 15% CO_2 was used with an optimum flow rate. The welding parameters used for carrying out the welding is given in Table 1.

Subsequently, different header to stub joints could be successfully welded using the optimised process parameters.

Figure 4 - Penetration achieved for different CTWD

Table 1 - Welding Parameters

S. No.	Mode	Current	Voltage	Pass
1.	Force Arc	260-280	27-29	Root Pass
2.	Force Arc	210-230	24-25	Filler Pass - 2

3.0 Results and Discussion

The inherent nature of the Force Arc process with long electrode extension and high preheating of the wire electrode gives higher deposition rate. Also, this deep penetration arc mode is more resistive to porosity due to dynamic arc and quick freezing weld. A resulting constant arc length control demonstrating the ability to fine tune the system to adjust to random variations in CTWD with changing of the arc length. The welding current used is also normally much higher than for normal short circuit transfer welding. This permits higher travel speed and results in better penetration profile.

Macrostructural analysis of the header to stub joint shows full penetration (Fig. 6) could be achieved by the Force Arc process. On ensuring the results through macrostructures, hydro testing has been carried out on the mock up header-stub assembly (Fig. 7). The improved fusion and penetration characteristics of Force Arc process is particularly advantageous in root formation in this tight and narrow joint configurations. The penetration is much deeper in the Force Arc mode than with a normal spray arc, which will increase the productivity by increasing the number of stubs that can be welded per shift. The overall welding time has been reduced by reduced no. of layers and passes and also by avoiding slag removal, grinding, etc.

In the present application of welding stubs to the headers, the deep penetration mode with good

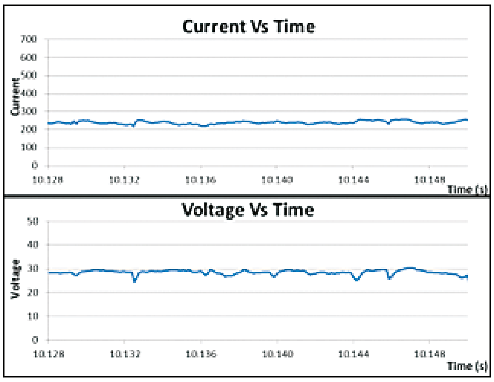

Figure 5 - Current and voltage signatures of advanced spray transfer

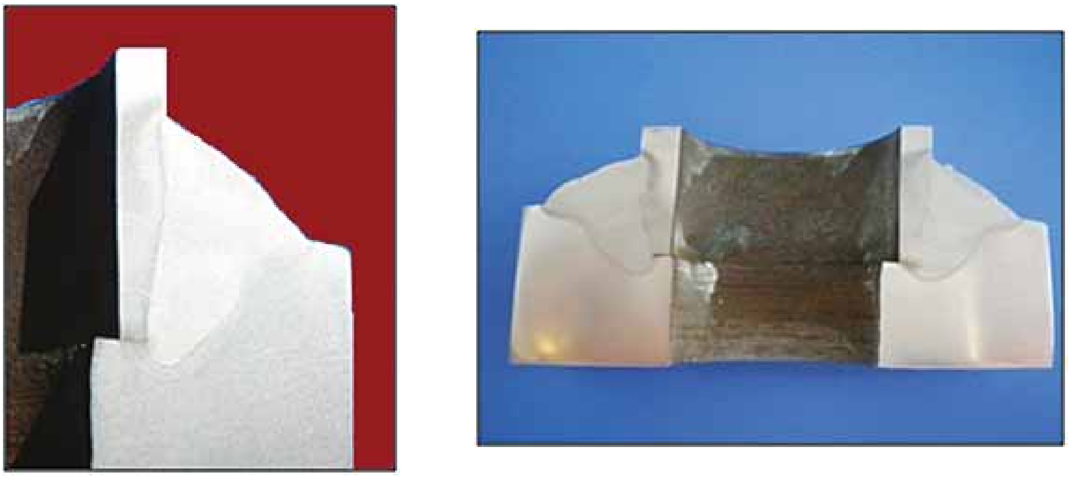

Figure 6 - Fusion joint by deep penetration process

Figure 7 - Hydro test on mock up header

fusion characteristics will be beneficial. In conventional GMAW power sources, spray mode of metal transfer with high arc voltage and amperage will be required as depicted in Fig.3, which may divert the arc by the arc blow leading to risk of undercuts and pores. In addition, the chances of melting loss of alloy elements may occur. For the stub welding application, it requires a very short arc with longer short circuit phases, since the torch has to be taken to the distance of minimum of 12 mm to reach the root of the stub profile. To achieve this, it requires a power source which will deliver the required voltage and current to reach the stub root. Also, it would be required to have either a torch, which travels upto the depth of the stub or the process which will deliver the desired parameters to ignite the arc even at longer contact to tube distance. With modern digital control power sources, it became possible to intervene in the process at a fast control speed with a very short arc and with longer short-circuit phases. The current is run down very quickly on re-ignition until the programmed nominal arc voltage is reached. (Fig. 5). This drastically reduces the power time period of the short-circuit phase and reduces the spatter formation to a tenable minimum.

In conventional spray mode or short circuit mode, increase of standoff distance will decrease the current and also, it will have an impact on the quality by means of porosity. In deeper penetration mode, the variation in stand-off distance did not affect the fusion as well penetration, as seen earlier. This is an excellent feature for providing defect-free welds both in manual and mechanized welding applications, which reduces the arcing

 

Figure 8 - Productionisation trials

time by way of minimised number of passes and non-arcing time by elimination of slag removal.

Finally, this advanced GMAW process has been successfully implemented by welding header made of SA335 P12 and pipe of Dia. 355.6 x 80 mm with 132 stubs of Dia. 38.1 x 6.6 mm& (Straight end stub) & 38.1 x 9.65 mm (Taper End)-24 Nos. made of SA 213 T 12 material. MPI has been done on all the welded joints and were found to be acceptable. Hydro testing has been carried out at a pressure of 450.9 kg/cm^2 and the fabricated header passed the hydro successfully.

4.0 Conclusion:

Waveform controlled power sources offer possibility of achieving deep penetration for header to stub tube welding. With its inherent feature of self-adjustable arc, the gas shielded metal arc welding with advanced spray transfer technique blend with intelligent control will offer the greater advantage of producing longer short circuit - short arc pulses. In deeper penetration mode the variation in stand-off distance did not affect the fusion as well penetration. This new variant of the power source technology enabled to produce deep penetration joints at shop floor to enhance the quality, reliability and availability of boilers.

This development has resulted in improved weld quality, productivity as well as reduced process time. The repeatability and quality of joints are ensured through newly developed welding procedure. The introduction of this technology adds for the use of state of art technology in turning out products with enhanced and consistent quality.

References:

1. **Larry Jeffus,** "Welding principles and applications – 7th Edition",2012.
2. **Tyrone L. Vincent,** "Waveform control in welding power supplies", IEEE Control Systems (Volume: 26, Issue: 4, Aug. 2006) Page(s): 17 – 18.
3. **Paul Kah, RaimoSuoranta, J.Martikainen July,** "Advanced gas metal arc welding processes"International Journal of Advanced Manufacturing Technology, Vol. 67(1):655-674, 2013.
4. **Hermans MJM, Den OG,** "Process behavior and stability in short circuit gas metal arc welding." Welding Journal 78(4): 137–141, 1999.

WELDING METALLURGY OF DUPLEX STAINLESS STEEL DURING RESISTANCE SPOT WELDING

This paper investigates the metallurgical and mechanical response of 2304 duplex stainless steel as an interesting candidate for automotive body in white applications to resistance spot welding. The results showed the high cooling rate associated with the resistance spot welding process suppressed the post solidification ferrite austenite transformation leading to improper ferrite austenite phase balance with a reduced volume fraction of austenite and consequent precipitation of chromium rich nitrides. The effects of welding current, as the key parameter determining the weld heat input, on the austenite volume fraction and precipitation are discussed. The minimum fusion zone hardness corresponding to the highest austenite volume fraction and minimum volume fraction of nitrides was obtained when the cooling rate was the lowest. The failure mode transition, peak load, and energy absorption of the welds were investigated. It was found that the fusion zone size is the key factor controlling peak load and energy absorption of the welds. Mechanical properties of the duplex stainless steel spot welds were compared with those of other automotive steels.

Welding Journal, V.96, Number.09, Sep 2017, page 307-s

IMPROVED FORMABILITY OF FUSION WELDED AA5182O ALUMINUM TAILOR WELDED BLANKS

There is an industry wide desire to produce aluminum alloy tailor welded blanks for automotive applications to facilitate light weighting of automotive body structures; however, the ductility and formability of blanks made using conventional fusion welding processes have not yet been acceptable due to the effects of internal and surface weld defects. The objective of this study was to identify techniques that might be used to reduce weld defects and improve ductility and formability in autogenous fusion welded AA5000 series aluminum tailor welded blanks. The double sided arc welding (DSAW) process was used to produce autogenous welds between 1.0and 1.5mm thick AA5182O aluminum sheets. While visually acceptable conduction mode DSAW welds could be made using a range of powers and welding speeds, weld metal ductility and formability were not acceptable due to the presence of internal weld defects including hydrogen porosity, solidification micro porosity, and solidification porosity and cracking at the weld center line. A comprehensive set of techniques was developed that minimized the occurrence of these weld defects. The resulting defect free fusion welds were found to have significantly improved ductility and formability with final fracture occurring in the thin sheet of the tailor welded blank and not in the fusion weld.

Welding Journal, V.96, Number.09, Sep 2017, page 319-s

PROCESS MONITORING OF RESISTANCE SPOT WELDING USING THE DYNAMIC RESISTANCE SIGNATURE

The quality of resistance spot welds used to manufacture automobiles is critical to their safety. Monitoring of spot welds during production is, therefore, a high priority for ensuring quality control. Interactions between the mechanical, thermal, and electrical processes involved in resistance spot welding (RSW) make the prediction of weld quality difficult. This complexity is confounded by the changing process variables in RSW that must be monitored in process to monitor the quality of spot welds, such as electrode wear, physical setup, and surface contamination. This paper presents a complete process monitoring method for RSW, including models for weld quality and process condition. Information is extracted from the dynamic resistance signature (DRS) collected during welding. The method allows for quick, inline detection of faults, identification of the responsible variables, and diagnosis of the cause of the abnormal behavior without requiring parts to be removed from the production line

Welding Journal, V.96, Number.11, Nov 2017, page 403-s

EFFECT OF FLUXES ON METAL TRANSFER AND ARC LENGTH IN SAW

The effect of fluxes on metal transfer and arc length in submerged arc welding between500 and 1000 A for direct current electrode positive (DCEP) and alternating current (AC) polarity was captured in videos at 10,000 frames/s. Five fluxes were used with a 3.2mm wire: Lincoln weld® 760M, 980, and 880M; Lincoln ES200; and an experimental flux with 85% calcium fluoride. Under all the fluxes and currents tested, an arc was formed. Metal transfer at 500 A was in the form of an irregular shaped droplet formed under all fluxes and polarities, but more frequent explosions at the droplet surface were seen under the oxide fluxes compared to fluoride fluxes. Metal transfer between 600 and 1000 A DCEP showed a "whipping tail" under all the fluxes in DCEP, while in AC, the detachment morphology was different between the electrode positive (EP) and electrode negative (EN) cycle. The detachment in EP was similar to DCEP, while in EN, explosions were more predominant. Approximately 74% of the detachments were during the EP cycle. In both DCEP and AC, the detachment frequency increased with current. In DCEP, the oxide fluxes showed a higher detachment frequency than the fluoride fluxes; in AC, no obvious trend in detachment frequency was observed among the different fluxes. Fluoride fluxes exhibited a shorter arc length and more frequent short circuit events than the oxide fluxes. A higher average wire feed speed in DCEP was observed for high fluoride fluxes with low magnesium oxide contents, suggesting that flux composition somehow increases anode fall voltage.

Welding Journal, V.96, Number.09, Sep 2017, page 334-s

FALL VOLTAGES IN ADVANCED WAVEFORM ALUMINUM GMAW

Fall voltages were concurrently measured in aluminum gas metal arc welding (GMAW), giving increased insight and prediction capabilities. A solid state calorimeter and a water cooled cathode were used to determine the heat distribution in aluminium GMAW utilizing a 1.2mm (3⁄64in.) 4043 aluminum electrode with 100% Ar in direct current electrode positive polarity. Fall voltage, thermal efficiency, and droplet heat content were determined for constant voltage, constant power, pulse, constant current pulse, and pulse on pulse waveforms. Overall cathode fall voltage was independent from current and waveform selection. It was also lower than initially expected based on material work functions, indicating that arc composition and/or temperature may be influencing overall cathode fall voltage measurements. Overall anode fall voltage was independent from current and had slight variations with waveform selection. Contact tip and electrode extension fall voltage were proportional to current but small compared to other measurements. Arc column potential appeared to be independent of waveform selection but dependent on current. Comparative tests between the calorimetry setup and an aluminium plate indicated that the calorimeter is representative of metal transfer mode when arc length is sufficiently large. Predicting voltage loss and wire feed rates with measured fall voltages were found to agree reasonably well with empirical results. The measurements found will assist various models, giving a more complete understanding of the aluminum GMAW system for various welding waveforms.

Welding Journal, V.96, Number.09, Sep 2017, page 354-s

FAILURE MODE OF SPOT WELDS UNDER CROSS TENSION AND COACH PEEL LOADS

Two analytical models were proposed to predict the critical weld button size (governing the failure mode transform from interfacial failure to pullout failure) in the cross tension and coach peel tests, respectively. Three stack ups, i.e., 1.0/1.0/1.0, 1.5/1.5/1.5, and 2.0/2.0/2.0 mm were tested. The cross tension joint failed under the combined action of tensile stress and shear stress, while the coach peel joint almost failed under pure shear stress. The joint design had little effect on the critical weld button size because the stress state was the same at the micro level. The proposed analytical models can be used to predict the critical button size for three sheet 6061 and 5754 aluminum alloy resistance spot welds under cross tension and coach peel loads.

Welding Journal, V.96, Number.11, Nov 2017, page 413-s

ORBITAL HOT WIRE NARROW GAP GTAW SYSTEM

SPECIFICATIONS

- Power source – PC600
- Welding current: : 5-550 A
- Hot wire power Source
  - Current – 160 A @ 100%
- Welding head – Polycar MP with dual carriage for 15 kg spool size
- Wire feeder – 0.8 mm & 1.0 mm
- NG200 welding torch with and without weaving with dual camera
- Component stage
  - Pipe Diameter – 400 – 1200 mm
  - Weight – Four jaw chuck upto 5 tonnes

ADVANTAGES

- Similar and dissimilar pipe welding in 5G position
- Special feature to follow seam trajectory during welding
- Integrated dual camera with video recording option for online monitoring of both tungsten electrode and wire feeding
- Data acquisition system for recording, monitoring and studying the parameters
- Integrated welding position information for precise control of welding speed

APPLICATIONS

- High wall thickness pipe welding in 5G position
- Welding in narrow groove upto a wall thickness of 200 mm

बी एच ई एल BHEL

WELDING RESEARCH INSTITUTE
BHARAT HEAVY ELECTRICALS LIMITED
TIRUCHIRAPPALLI-620014

WRI

TRAINING PROGRAMMECALENDAR FOR THE YEAR 2018 – 2019

Sl. No	TITLE	CODE	COURSE DURATION
1	WELDING & INSPECTION	STC - 438	04.06.2018 – 09.06.2018
2	CERTIFIED WELDING INSPECTORS *	CWI - 113	04.06.2018 – 09.06.2018
3	WELDING & INSPECTION	STC - 439	09.07.2018 – 14.07.2018
4	CERTIFIED WELDING INSPECTORS *	CWI - 114	17.07.2018 – 28.07.2018
5	ULTRASONIC TESTING – LEVEL II *	NDT - 137	31.07.2018 – 11.08.2018
6	WELDING & INSPECTION	STC - 440	27.08.2018 – 01.09.2018
7	CERTIFIED WELDING INSPECTORS *	CWI - 115	04.09.2018 – 15.09.2018
8	WELDING & INSPECTION	STC - 441	24.09.2018 – 29.09.2018
9	RT FILM INTERPRETATION - LEVEL II*	NDT - 138	08.10.2018 – 13.10.2018
10	WELDING & INSPECTION	STC - 442	22.10.2018 – 27.10.2018
11	CERTIFIED WELDING INSPECTORS *	CWI - 116	13.11.2018 – 24.11.2018
12	NDT TECHNIQUES	NDT - 139	26.11.2018 – 30.11.2018
13	WELDING & INSPECTION	STC - 443	03.12.2018 – 08.12.2018
14	CERTIFIED WELDING INSPECTORS *	CWI - 117	11.12.2018 – 22.12.2018
15	WELDING & INSPECTION	STC - 444	07.01.2019 – 12.01.2019
16	CERTIFIED WELDING INSPECTORS *	CWI - 118	05.02.2019 – 16.02.2019
17	WELDING & INSPECTION ***	STC - 445	11.03.2019 – 16.03.2019

***** The course shall be organised if there is adequate number of registered Participants.**

*** Programme includes examination.**

- *All courses are "Non Residential"*
- WRI has conducted 1013 Welding & NDT Courses, so far, benefiting 20460 Engineers / Supervisors from private / public sector organisations apart from individuals, throughout the country and abroad.
- Under the technical skill development training programme, more than 6250 welders have been trained so far.
- In addition, for specific industries tailor-made programmes on topics related to welding & allied areas can be organised at WRI, on mutually agreed terms
- Bachelor accommodation (Shared) at Guest House is available for course participants on payment, subjected to availability.

For your requirements, please contact: -
***Phone No.:* 0431-2577283 / 2577433 / 2577344 *Fax No.:* 0431-2520773**
E-mail: **kkganesh@bhel.in / wrisow@bhel.in** Website: **www.wriindia.com**

- Forty third year of service in the field of welding and allied areas
- Developed and Commercialised more than 50 products / technologies
- Has filed more than 162 patents (Granted-40)
- Served more than 1000 industries in different sectors
- More than 1125 technical papers in national and international journals and conference and 75 awards won
- Has a Memorandom of Understanding with German Welding Institute (DVS) for joint working
- An Agreement on Collaborative Research and Exchange with JWRI, the Japanese Joining and Welding Research Institute.
- A Protocol of Intention signed with University of Hannover, Germany.
- Trained more than 25200 welding personnel through various training programmes
- A reference book on "Industrial welding technology" authored by WRI published by Central Instructional Media Institute (CIMI). Chennai for practising welding personnel
- Important research work carried out in the Institute published in "WRI Journal"
- Recognised by DSIR as a national research facility
- Recognised by DST for training and certification of welders
- Approved by Central Boilers Board for certification of welders as per IBR
- Recognised centre for Doctoral Research (IITs, IISc, NIT & Anna University)
- Approved by NHPC for certification of welding consumables
- Recognised by Industries from Middle East (Dubai, Oman, Sri Lanka, Bhutan and UAE) for training & certification of welding personnel as per international standards.
- Winner of SKOCH - BSE Award 2016

FOR SOLUTIONS PAR EXCELLENCE CONTACT:

बी एच ई एल
BHEL

THE HEAD
WELDING RESEARCH INSTITUTE
BHARAT HEAVY ELECTRICALS LIMITED
TIRUCHIRAPPALLI - 620 014
Tel: +91 431 - 2577506, Fax: +91 431 - 2576824

WRI

E - mail : wri@bheltry.co.in
Website: www.wriindia.com

Design & Printed by: M/s. Poornima Printers
Bengaluru. Ph : 23359588